The Interaction Picture method for solving the generalized nonlinear Schrödinger equation in optics

Stéphane Balac, Arnaud Fernandez, Fabrice Mahé, Florian Méhats, Rozenn Texier-Picard

THE INTERACTION PICTURE METHOD FOR SOLVING THE GENERALIZED NONLINEAR SCHRÖDINGER EQUATION IN OPTICS

STÉPHANE BALAC[†¶], ARNAUD FERNANDEZ[†], FABRICE MAHÉ[‡], FLORIAN MÉHATS[‡], AND ROZENN TEXIER-PICARD[§]

Abstract. The "interaction picture" (IP) method is a very promising alternative to Split-Step methods for solving certain type of partial differential equations such as the nonlinear Schrödinger equation involved in the simulation of wave propagation in optical fibers. The method exhibits interesting convergence properties and is likely to provide more accurate numerical results than cost comparable Split-Step methods such as the Symmetric Split-Step method. In this work we investigate in detail the numerical properties of the IP method and carry out a precise comparison between the IP method and the Symmetric Split-Step method.

Key words. Interaction Picture method, Symmetric Split-Step method, Runge-Kutta method, Nonlinear optics, nonlinear Schrödinger equation.

AMS subject classifications. 65M12, 65M15, 65L06, 65T50, 78A60

1. Introduction. In this paper we study a mathematical model for the propagation of optical pulses into a single-mode fiber. We make the following usual assumptions, see for example [1] for a justification:

- the optical wave is assumed to be quasi-monochromatic, i.e. the spectral width of the pulse spectrum is small compared to the mean pulsation ω_0;
- the optical wave is supposed to maintain its polarization along the fiber length so that a scalar model (rather than a full vectorial one) is valid;
- the electric field $\mathbf{E}$ is linearly polarized along a direction $\mathbf{e_x}$ transverse to the direction of propagation $\mathbf{e_z}$ defined by the fiber axis and can be represented as a function of time τ and position $\mathbf{r} = (x, y, z)$ as

$$\mathbf{E}(\mathbf{r}, \tau) = A(z, \tau)\, F(x, y)\, \mathrm{e}^{-\mathrm{i}(\omega_0 \tau - kz)}\ \mathbf{e_x}$$

  where $A(z, \tau)$ represents the slowly varying pulse envelope, $F(x, y)$ is the modal distribution and k is the wavenumber. The pulse envelope $A(z, \tau)$ is expressed in a frame of reference, called the *retarded frame*, moving with the pulse at the "group velocity" $v_g = c/n_g$. The relation between the "local time" t in the retarded frame and the absolute time τ is: $t = \tau - z/v_g$.

Under these assumptions, the evolution of the slowly varying pulse envelope A is governed by the Generalized Nonlinear Schrödinger Equation (GNLSE) [1]

$$\frac{\partial}{\partial z} A(z,t) = -\frac{\alpha}{2} A(z,t) + \left(\sum_{n=2}^{N} \mathrm{i}^{n+1} \frac{\beta_n}{n!} \frac{\partial^n}{\partial t^n} A(z,t) \right) \tag{1.1}$$

$$+ \mathrm{i}\gamma \left(\mathrm{I_d} + \frac{\mathrm{i}}{\omega_0} \frac{\partial}{\partial t} \right) \left[A(z,t) \Big((1 - f_R)\, |A(z,t)|^2 + f_R \int_{-\infty}^{+\infty} h_R(s) |A(z, t-s)|^2 \, \mathrm{d}s \Big) \right]$$

[†]FOTON UMR 6082, Université de Rennes I, CNRS, UEB, Enssat, 6 rue de Kerampont, CS 80518, 22305 Lannion, France

[‡]IRMAR, Université de Rennes I, CNRS, UEB, Campus de Beaulieu, 35042 Rennes, France

[§]IRMAR, ENS Cachan Bretagne, Université de Rennes I, CNRS, UEB, avenue Robert Schuman, 35170 Bruz, France

[¶]This work has been undertaken under the framework of the Green-Laser project and was partially supported by Conseil Régional de Bretagne, France.

where $\mathrm{I_d}$ denotes identity operator. The physical effects taken into account in (1.1) are the following. First, some linear effects are expressed through the linear attenuation/gain coefficient α and the linear dispersion coefficients β_n, $2 \leq n \leq N$ (it is assumed that $\beta_N \neq 0$), where e.g. β_2 expressed in units $\mathrm{ps^2 km^{-1}}$ accounts for chromatic effects. In standard silica fibers we have $\alpha \sim 4.0\,10^{-2}\,\mathrm{km^{-1}}$ and $\beta_2 \sim 50\,\mathrm{ps^2 km^{-1}}$ for wavelengths in the visible region. In the anomalous dispersion regime we have $\beta_2 < 0$ (typically $\beta_2 \sim -20\,\mathrm{ps^2 km^{-1}}$ for wavelengths near $1.5\,\mu\mathrm{m}$) and the fiber can support optical soliton. Nonlinear effects are involved through the nonlinear parameter γ with typical values in the range 1 to $10\,\mathrm{W^{-1} km^{-1}}$. In (1.1), first order partial derivation with respect to time takes into account the dispersion of the nonlinearity through the simplified optical shock parameter $\tau_{\mathrm{shock}} = 1/\omega_0$. Instantaneous Kerr effect manifests itself through the term $(1 - f_R)\,|A|^2$. The delayed Raman contribution in the time domain is taken into account through the convolution product between the instantaneous power $|A|^2$ and the Raman time response function h_R. For silica fibers, an expression for h_R is proposed in [1]. The constant f_R represents the fractional contribution of the delayed Raman response to nonlinear polarization and takes a value around 0.2. Equation (1.1) does not take into account other physical phenomena such as amplified spontaneous emission and Raman spontaneous emission. Our interest for the GNLSE originates from a study of pulsed laser systems of MOPFA type (a master oscillator coupled with fiber amplifier usually a cladding-pumped high-power amplifier based on an ytterbium-doped fiber), see [15] for details. The PDE (1.1) is to be solved for all z in a given interval $[0, L]$ where L denotes the length of the fiber and for all "local time" $t \in \mathbb{R}$. It is considered together with the following boundary condition $A(0, t) = a_0(t)\ \forall t \in \mathbb{R}$, where a_0 is a given complex valued function.

1.1. Mathematical toolbox. Recently a "fourth-order Runge-Kutta method in the interaction picture method" (RK4-IP method) has been proposed in [20] as an alternative to Split-Step methods for solving the GNLSE (1.1). The method has been numerically experimented on benchmark problems in optics in [20, 19]. The scope of the present work is to investigate the mathematical features of the RK4-IP method for solving the GNLSE. The mathematical study of equation (1.1) itself and the set up of the corresponding functional framework for the study of the RK4-IP method is arduous due to the complicated expression of the nonlinear part of the equation. For this reason, to proceed with the mathematical justification of the RK4-IP method and its numerical analysis, we will consider the following simplified version of equation (1.1), corresponding to $\omega_0 = +\infty$ and $f_R = 0$ (still the numerical tests in Section 3.3 are done with the general model $\omega < +\infty$, $f_R > 0$),

$$\frac{\partial}{\partial z} A(z) = -\frac{\alpha}{2} A(z) + \left(\sum_{n=2}^{N} \mathrm{i}^{n+1} \frac{\beta_n}{n!} \frac{\partial^n}{\partial t^n} A(z) \right) + \mathrm{i}\gamma A(z) |A(z)|^2, \tag{1.2}$$

where the notation $A(z)$ stands for the first partial function of A in z, i.e. $A(z) : t \in \mathbb{R} \mapsto A(z, t) \in \mathbb{C}$. In (1.2), the nonlinear part is actually similar to the one involved in the standard nonlinear Schrödinger (NLS) equation in optics [1]

$$\frac{\partial}{\partial z} A(z) = -\frac{\alpha}{2} A(z) - \frac{\mathrm{i}}{2} \beta_2 \frac{\partial^2}{\partial t^2} A(z) + \mathrm{i}\gamma\, A(z)\, |A(z)|^2 . \tag{1.3}$$

We denote by $\mathbb{L}^p(\mathbb{R}, \mathbb{C})$, $p \in [1, +\infty[$ the set of complex-valued functions over $\mathbb{R}$ whose p-th powers are integrable and by $\mathbb{H}^m(\mathbb{R}, \mathbb{C})$ for $m \in \mathbb{N}^*$ the Sobolev set of functions in $\mathbb{L}^2(\mathbb{R}, \mathbb{C})$ with derivatives up to order m in $\mathbb{L}^2(\mathbb{R}, \mathbb{C})$. For convenience, we will also use the notation $\mathbb{H}^0(\mathbb{R}, \mathbb{C})$ for $\mathbb{L}^2(\mathbb{R}, \mathbb{C})$ and $\mathbb{L}^\infty(\mathbb{R}, \mathbb{C})$ for the space of essentially bounded functions. The Sobolev spaces $\mathbb{H}^m(\mathbb{R}, \mathbb{C})$, $m \in \mathbb{N}$, are equipped with the usual norms denoted $\| \ \|_m$. For $k, n \in \mathbb{N}$ and $I \subset \mathbb{R}$, we denote by $\mathcal{C}^k(I; \mathbb{H}^n(\mathbb{R}, \mathbb{C}))$ the space of functions $u : z \in I \mapsto u(z) \in$

$\mathbb{H}^n(\mathbb{R},\mathbb{C})$ with continuous derivatives up to order k (or just continuous when $k=0$). For any $m\in\mathbb{N}$ and any interval $I\subset\mathbb{R}$, we define

$$E_{m,N}(I)=\bigcap_{k=0}^{\lfloor m/N\rfloor}\mathcal{C}^k(I,\mathbb{H}^{m-Nk}(\mathbb{R},\mathbb{C})), \tag{1.4}$$

where $\lfloor s\rfloor$ denotes the integer part of $s\in\mathbb{R}_+$.

A comprehensive mathematical framework for the NLS equation (1.3) exists in the literature [8, 9]. Namely, it is known that for $a_0\in\mathbb{H}^2(\mathbb{R},\mathbb{C})$ there exists a unique A belonging to $\mathcal{C}^0(\mathbb{R};\mathbb{H}^2(\mathbb{R},\mathbb{C}))\bigcap\mathcal{C}^1(\mathbb{R};\mathbb{L}^2(\mathbb{R},\mathbb{C}))$ solution of equation (1.3) satisfying $A(0)=a_0$. This result can be extended to the GNLSE with $\omega_0=+\infty$ and $f_R=0$, i.e. to (1.2), as follows.

THEOREM 1.1. *For all $a_0\in\mathbb{H}^m(\mathbb{R},\mathbb{C})$, with $m\in\mathbb{N}^*$, there exists a unique maximal solution $A\in E_{m,N}([0,Z[)$, with $Z\in]0,+\infty]$, to the problem* (1.2). *This solution satisfies*

$$\|A(z)\|_0=\mathrm{e}^{-\frac{\alpha}{2}z}\,\|a_0\|_0\qquad\text{for all } z\in[0,Z[\tag{1.5}$$

and it is maximal in the sense that

$$\text{if}\quad Z<+\infty\quad\text{then}\quad\limsup_{z\to Z}\|A(z)\|_{\mathbb{L}^\infty}=+\infty. \tag{1.6}$$

Moreover, if N is even and $m\geq N/2$ then the solution is global, i.e. $Z=+\infty$.

The proof of this result can be found in Appendix A.

In order to simplify the presentation of the interaction method, we will now reformulate our problems (1.1) and (1.2) in a more abstract and unified way. To this aim, we need a few notations and technical results. We denote by $\mathcal{D}$ the unbounded linear operator on $\mathbb{L}^2(\mathbb{R},\mathbb{C})$ with domain $\mathbb{H}^N(\mathbb{R},\mathbb{C})$, $N\in\mathbb{N}^*$, defined as

$$\mathcal{D}:U\in\mathbb{H}^N(\mathbb{R},\mathbb{C})\longmapsto\sum_{n=2}^{N}\mathrm{i}^{n+1}\frac{\beta_n}{n!}\frac{\partial^n}{\partial t^n}U\in\mathbb{L}^2(\mathbb{R},\mathbb{C}).$$

For $N=2$, it is well known [8, 9] that this operator generates a continuous group of bounded operators on $\mathbb{L}^2(\mathbb{R},\mathbb{C})$, denoted by $\exp(z\mathcal{D})$ with $z\in\mathbb{R}$. For $N>2$, the same property holds and we have the following lemma.

LEMMA 1.2. *Let $\varphi\in\mathbb{H}^m(\mathbb{R},\mathbb{C})$, where $m\in\mathbb{N}$. Then the problem*

$$\frac{\partial}{\partial z}U(z)=\mathcal{D}U(z)\quad\forall z\in\mathbb{R},\qquad U(0)=\varphi \tag{1.7}$$

has a unique solution $U(z)=\exp(z\mathcal{D})\varphi$ with $U:z\in\mathbb{R}\mapsto U(z)\in E_{m,N}(\mathbb{R})$ and it satisfies for all $z\in\mathbb{R}$ the relations $\|U(z)\|_j=\|\varphi\|_j$ for all $j\in\{0,\dots,m\}$.

Let us now denote the two nonlinear operators appearing respectively in the full GNLSE (1.1) and its simplified version (1.2) by

$$\mathcal{N}:u\longmapsto-\frac{\alpha}{2}u+\mathrm{i}\gamma\left(\mathrm{I_d}+\frac{\mathrm{i}}{\omega_0}\frac{\partial}{\partial t}\right)\left[(1-f_R)u|u|^2+f_Ru\int_{-\infty}^{+\infty}h_R(s)|u(\cdot-s)|^2\,\mathrm{d}s\right]$$

and

$$\mathcal{N}_0:u\longmapsto-\frac{\alpha}{2}u+\mathrm{i}\gamma\,u|u|^2.$$

Both $\mathcal{N}$ and $\mathcal{N}_0$ are considered as unbounded nonlinear operators on $\mathbb{L}^2(\mathbb{R},\mathbb{C})$. Note that $\mathcal{N}_0$ is nothing but $\mathcal{N}$ when $\omega_0 = +\infty$ and $f_R = 0$. Problems (1.1) and (1.2) then can be reformulated respectively as

$$\frac{\partial}{\partial z}A(z) = \mathcal{D}A(z) + \mathcal{N}(A)(z) \quad \forall z \in \mathbb{R}, \qquad A(0) = a_0 \tag{1.8}$$

and

$$\frac{\partial}{\partial z}A(z) = \mathcal{D}A(z) + \mathcal{N}_0(A)(z) \quad \forall z \in \mathbb{R}, \qquad A(0) = a_0. \tag{1.9}$$

It can be useful to note that another splitting is possible for $\mathcal{D}$ and $\mathcal{N}$: the term $-\frac{1}{2}\alpha A(z)$ can be added to the linear operator instead of the nonlinear one.

As we said above, the numerical experiments presented below are done on (1.1) (or equivalently, (1.8)), but the mathematical results concern the simplified problem (1.2) (or equivalently, (1.9)). Indeed, due to the time derivative, the nonlinearity $\mathcal{N}$ is not continuous on any Sobolev space (unless $\omega_0 = +\infty$) and the resolution of the Cauchy problem for (1.1) would rely on the smoothing properties of the linear group connected to the higher-order dispersion, which goes beyond the scope of this paper on a numerical method. Instead, the simplified nonlinearity $\mathcal{N}_0$ is Lipschitz continuous on every Sobolev space $\mathbb{H}^m$ of exponent $m \geq 1$. We recall indeed that for all $q \in [2,+\infty]$ we have the inclusion $\mathbb{H}^1(\mathbb{R},\mathbb{C}) \subset \mathbb{L}^q(\mathbb{R})$ and we summarize in the following lemma (stated without proof, see [7]) some classical useful properties of $\mathcal{N}_0$:

LEMMA 1.3. *The nonlinear operator $\mathcal{N}_0$ satisfies a local Lipschitz conditions in any $\mathbb{H}^m(\mathbb{R},\mathbb{C})$, $m \geq 1$: for all $M > 0$ and $m \in \mathbb{N}^*$, there exists $\Lambda_{m,M} > 0$ such that, for all $u, v \in \mathbb{H}^m(\mathbb{R},\mathbb{C})$ such that $\|u\|_m \leq M$ and $\|v\|_m \leq M$, we have*

$$\|\mathcal{N}_0(u) - \mathcal{N}_0(v)\|_m \leq \Lambda_{m,M} \, \|u - v\|_m .$$

Moreover for all $m \in \mathbb{N}^*$ we have $\mathcal{N}_0 \in \mathcal{C}^\infty(\mathbb{H}^m(\mathbb{R},\mathbb{C}), \mathbb{H}^m(\mathbb{R},\mathbb{C}))$.

1.2. Presentation of the numerical approach. We describe here the "fourth-order Runge-Kutta method in the interaction picture method" (RK4-IP method) proposed in [20] as an alternative to Split-Step methods for solving the GNLSE (1.1). The experimental investigation undertaken in [20] on benchmark problems in optics indicates that the RK4-IP method exhibits interesting convergence properties and provides more accurate numerical results than comparable Split-Step methods such as the Symmetric Split-Step method based on Strang formula [29]. The main idea of the Interaction Picture (IP) method is a change of unknown to transform the NLSE or GNLSE for the unknown A into a new equation where only remains an explicit reference to the partial derivation with respect to the space variable z and where the time variable t appears as a parameter. This new equation can be solved numerically, using the usual methods for ordinary differential equations (ODE) such as the standard fourth order Runge-Kutta (RK4) method. Then, by using the inverse transform we obtain the approximate values of the unknown A at the grid points of a subdivision of the fiber length interval $[0, L]$. This numerical approach is referred to as the RK4-IP method.

The RK4-IP method has been developed by the Bose-Einstein condensate theory group of R. Ballagh from the Jack Dodd Centre at the University of Otago (New Zealand) in the 90's for solving the Gross-Pitaevskii equation which is ubiquitous in Bose condensation. It was described in the Ph.D. thesis of B. M. Caradoc-Davies [6] and M. J. Davis [11]. In this latter work an embedded Runge-Kutta scheme based on a Cash-Krap formula was additionally used in conjunction with the RK4-IP method for adaptive step-size control purposes but

the efficiency of the method was judged disappointing. However, the RK4-IP method has been widely used for numerical studies concerning Bose-Einstein condensates, see e.g. [32, 27, 21]. Recently an efficient embedded RK method based on Dormand and Prince RK4(3)-T formula [12] and specifically designed for the IP method has been proposed in [3]. The name "Interaction Picture" and the change of unknown at the heart of the method originate from quantum mechanics [30, 17] where it is usual to chose an appropriate "picture" in which the physical properties of the studied system can be easily revealed and the calculation made simpler. The interaction picture is considered as an intermediate between the Schrödinger picture and the Heisenberg picture. It is useful in quantum optics for solving problems with time-dependent Hamiltonians in the form $H(t) = H_0 + V(t)$ where H_0 is a Hamiltonian independent of the time and its eigenvalues are easy to compute whereas V is a time-dependent potential which can be complicated.

The RK4-IP method can be interpreted as an exponential Runge-Kutta method according to the general form presented in [24] for the semi-linear parabolic problems, but this method is not of collocation type as studied in [23] for parabolic problems and in [13] for the Schrödinger equation.

In this work we investigate the numerical properties of the RK4-IP method for the Generalized Nonlinear Schrödinger Equation, and we make a precise comparison between the RK4-IP method and the symmetric Split-Step Fourier method when used with the classical fourth-order Runge-Kutta formula (S3F-RK4 method). At present time, the S3F-RK4 method is the most widely used method for simulating wave propagation in optical fibers, see e.g. [1, 28, 31, 25]. We show that both methods are equivalent regarding the numerical cost, due to similar computational inner structures, but the RK4-IP method exhibits a convergence rate of order h^4 where h denotes the spatial discretisation step-size whereas the S3F-RK4 method is limited by the second order accuracy of Strang splitting formula and exhibits a convergence rate of order h^2.

The outline of the document is the following. In Section 2 we present the IP method, we detail the various aspects of the numerical implementation of the RK4-IP method and we analyze the numerical error of the method. Our main result is stated in Theorem 2.5. In Section 3, we present in a similar way the S3F-RK4 method and we compare the two methods both from a theoretical point of view (Proposition 3.1) and on numerical simulation examples.

2. Solving the GNLSE by the Interaction Picture method.

2.1. The idea of the Interaction Picture. The integration interval, say $[0, L]$, is divided into K subintervals where the spatial grid points are denoted z_k, $k \in \{0, \dots, K\}$ such that $]0, L] = \cup_{k=0}^{K-1}]z_k, z_{k+1}]$ where $0 = z_0 < z_1 < \cdots < z_{K-1} < z_K = L$. For convenience we assume a constant grid spacing $h = L/K$ but this assumption is not a limitation of the method and an adaptive step-size version of the RK4-IP method is propounded in [3]. For $k \in \{0, \dots, K\}$ we set $z_{k+\frac{1}{2}} = z_k + \frac{h}{2}$.

We introduce the following auxiliary problems, for $0 \leq k \leq K-1$:

$$\frac{\partial}{\partial z} A_k(z) = \mathcal{D} A_k(z) + \mathcal{N}(A_k)(z) \quad \forall z \in [z_k, z_{k+1}], \qquad A_k(z_k) = a_k \tag{2.1}$$

where a_k is a given function in $\mathbb{H}^m(\mathbb{R}, \mathbb{C})$. Solving problem (1.8) for $a_0 \in \mathbb{H}^m(\mathbb{R}, \mathbb{C})$ is equivalent to solving the sequence of connected problems (2.1), $k \in \{0, \dots, K-1\}$, with for all $k \in \{1, \dots, K-1\}$ $a_k(t)$ defined for all $t \in \mathbb{R}$ by $a_k(t) = A_{k-1}(z_k, t)$, and for all $k \in \{0, \dots, K-1\}$,

$$\forall z \in [z_k, z_{k+1}] \quad A(z) = A_k(z).$$

For $z, \zeta \in [z_k, z_{k+1}]$ and $t \in \mathbb{R}$, we denote by Ψ the mapping defined by

$$\Psi(z, \zeta, t) = \exp(-(\zeta - z_{k+\frac{1}{2}})\mathcal{D})A_k(z, t).$$

For a fixed value of z, the mapping $(\zeta, t) \mapsto \Psi(z, \zeta, t)$ coincides with the solution of the problem

$$\frac{\partial}{\partial \zeta} A(\zeta) = -\mathcal{D}A(\zeta) \quad \forall \zeta \in [z_k, z_{k+1}], \qquad A(z_{k+\frac{1}{2}}) = A_k(z).$$

For solving problem (2.1) we introduce as new unknown the mapping A_k^{ip} defined for $(z, t) \in [z_k, z_{k+1}] \times \mathbb{R}$ by $A_k^{\mathrm{ip}}(z, t) = \Psi(z, z, t)$, *i.e.*

$$A_k^{\mathrm{ip}} : (z, t) \in [z_k, z_{k+1}] \times \mathbb{R} \longmapsto \exp(-(z - z_{k+\frac{1}{2}})\mathcal{D})A_k(z, t) \in \mathbb{C}. \tag{2.2}$$

From Lemma 1.2, it can be deduced that $A_k \in E_{m,N}([z_k, z_{k+1}])$ is equivalent to $A_k^{\mathrm{ip}} \in E_{m,N}([z_k, z_{k+1}])$, where the space $E_{m,N}$ is defined by (1.4). Moreover, from the chain rule we have

$$\begin{aligned} \frac{\partial}{\partial z} A_k^{\mathrm{ip}}(z, t) &= \partial_1 \Psi(z, z, t) + \partial_2 \Psi(z, z, t) \\ &= \exp(-(z - z_{k+\frac{1}{2}})\mathcal{D}) \frac{\partial}{\partial z} A_k(z, t) - \mathcal{D} \exp(-(z - z_{k+\frac{1}{2}})\mathcal{D})A_k(z, t), \end{aligned} \tag{2.3}$$

where ∂_i denotes the derivative with respect to the i-th position variable. This enables to reformulate the GNLSE in the Interaction Picture.

For all $k \in \{0, \ldots, K-1\}$, if A_k solves (2.1) then A_k^{ip} defined in (2.2) satisfies

$$\frac{\partial}{\partial z} A_k^{\mathrm{ip}}(z) = \mathcal{G}_k(z, A_k^{\mathrm{ip}}(z)) \quad \forall z \in [z_k, z_{k+1}], \qquad A_k^{\mathrm{ip}}(z_k) = \exp(-(z_k - z_{k+\frac{1}{2}})\mathcal{D})a_k, \tag{2.4}$$

where $\mathcal{G}_k$ is defined by

$$\mathcal{G}_k(z, v) = \exp(-(z - z_{k+\frac{1}{2}})\mathcal{D}) \left[\mathcal{N} \left(\exp((z - z_{k+\frac{1}{2}})\mathcal{D})v \right) \right]. \tag{2.5}$$

Conversely, if A_k^{ip} is solution to (2.4) then $A_k = \exp((z - z_{k+\frac{1}{2}})\mathcal{D})A_k^{\mathrm{ip}}$ is solution to (2.1). At this level of generality, this statement is formal. However, in the case $\omega_0 = +\infty$, $f_R = 0$, since $\mathcal{N}$ reduces to $\mathcal{N}_0$, we shall see in Section 2.3 that the mapping $\mathcal{G}_k$ is continuous on $E_{m,N}$ and then that both formulations are equivalent (see in particular Lemma 2.2).

Remark 1. In the above presentation, it is possible to choose any point in the interval $[z_k, z_{k+1}]$ instead of the middle point $z_{k+\frac{1}{2}}$, but as we will see later this particular choice is very relevant to save computations.

The major interest in doing the above transformation is that on the contrary to problem (2.1), the new problem (2.4) for the unknown A_k^{ip} does not anymore involve explicitly partial derivation with respect to the time variable t. Partial derivation with respect to time now occurs through the operators $\exp(\pm(z - z_{k+\frac{1}{2}})\mathcal{D})$. The problem (2.4) can be solved numerically using a standard quadrature scheme for ODE such as the classical 4th order Runge-Kutta method [5, 10]. Moreover, the initial condition for problem (2.4) is obtained by computing the mapping $\exp(-(z_k - z_{k+\frac{1}{2}})\mathcal{D})a_k$.

We can summarize the IP method for solving problem (1.8) in the following way. The fiber length $[0, L]$ is divided into subintervals $[z_k, z_{k+1}]$, $k \in \{0, \ldots, K-1\}$, and over each subinterval $[z_k, z_{k+1}]$ the following three nested problems are solved:

$$\frac{\partial}{\partial z} A_k^+(z) = \mathcal{D}A_k^+(z) \quad \forall z \in [z_k, z_{k+\frac{1}{2}}], \qquad A_k^+(z_k) = A_{k-1}(z_k), \tag{2.6}$$

where $A_{k-1}(z_k)$ represents the solution to (2.1) at grid point z_k computed at the previous step $k-1$;

$$\frac{\partial}{\partial z}A_k^{\rm ip}(z) = \mathcal{G}_k(z, A_k^{\rm ip}(z)) \quad \forall z \in [z_k, z_{k+1}], \qquad A_k^{\rm ip}(z_k, t) = A_k^{+}(z_{k+\frac{1}{2}}), \tag{2.7}$$

where $\mathcal{G}_k$ is defined by (2.5) and $A_k^{+}(z_{k+\frac{1}{2}}) = \exp(\frac{h}{2}\mathcal{D})A_{k-1}(z_k)$ is the solution to (2.6) at grid point $z_{k+\frac{1}{2}}$;

$$\frac{\partial}{\partial z}A_k^{-}(z) = \mathcal{D}A_k^{-}(z) \quad \forall z \in [z_{k+\frac{1}{2}}, z_{k+1}], \qquad A_k^{-}(z_{k+\frac{1}{2}}) = A_k^{\rm ip}(z_{k+1}), \tag{2.8}$$

where $A_k^{\rm ip}(z_{k+1})$ represents the solution to (2.7) at grid point z_{k+1}. Finally, at grid point z_{k+1}, the solution $A_k(z_{k+1})$ to (2.1) is given by $A_k^{-}(z_{k+1})$. The two linear PDE problems (2.6) and (2.8) can be numerically solved very efficiently by use of Fourier Transform as detailed in Section 2.2.2.

2.2. The fourth order Runge-Kutta scheme in the Interaction Picture method.

2.2.1. Approximating the solution to problem (2.7) by one RK4 step. For $k \in \{0, \dots, K-1\}$ we denote by $u_k^{\rm ip}$ (resp. u_k) the approximation of $A_k^{\rm ip}(z_k)$ (resp. $A_k(z_k)$) the solution to problem (2.7) (resp. (2.1)) at grid point z_k. One step of the classical 4th order Runge-Kutta formula is used to approximate the solution to problem (2.7) at grid point z_{k+1} as follows:

$$A_k^{\rm ip}(z_{k+1}) \approx u_{k+1}^{\rm ip} = u_k^{\rm ip} + h\,\Phi(z_k, u_k^{\rm ip}; h) \tag{2.9}$$

where the mapping Φ is the *increment function* of the RK4 method, defined by

$$\Phi(z_k, u_k^{\rm ip}; h) = \frac{h}{6}\left(\alpha_1 + 2\alpha_2 + 2\alpha_3 + \alpha_4\right)$$

with

$$\begin{aligned}
\alpha_1 &= \mathcal{G}_k(z_k, u_k^{\rm ip}) = \exp(\tfrac{h}{2}\mathcal{D})\mathcal{N}(\exp(-\tfrac{h}{2}\mathcal{D})u_k^{\rm ip}) \\
\alpha_2 &= \mathcal{G}_k(z_k + \tfrac{h}{2}, u_k^{\rm ip} + \tfrac{h}{2}\alpha_1) = \mathcal{N}(u_k^{\rm ip} + \tfrac{h}{2}\alpha_1) \\
\alpha_3 &= \mathcal{G}_k(z_k + \tfrac{h}{2}, u_k^{\rm ip} + \tfrac{h}{2}\alpha_2) = \mathcal{N}(u_k^{\rm ip} + \tfrac{h}{2}\alpha_2) \\
\alpha_4 &= \mathcal{G}_k(z_k + h, u_k^{\rm ip} + h\alpha_3) = \exp(-\tfrac{h}{2}\mathcal{D})\mathcal{N}(\exp(\tfrac{h}{2}\mathcal{D})[u_k^{\rm ip} + h\alpha_3])
\end{aligned} \tag{2.10}$$

Using the change of unknown (2.2) we deduce the following approximation of the solution to problem (2.1) at grid point z_{k+1}

$$A_k(z_{k+1}) \approx u_{k+1} = \exp(\tfrac{h}{2}\mathcal{D})\big(u_k^{\rm ip} + \tfrac{h}{6}\left(\alpha_1 + 2\alpha_2 + 2\alpha_3 + \alpha_4\right)\big). \tag{2.11}$$

Actually we are only interested in computing an approximate solution to problem (1.8) given by (2.11) and the use of the new unknown $A_k^{\rm ip}$ is a go-between in the computational approach. We can therefore recast the above approximation scheme in order to reduce the cost of the method as follows:

$$\begin{aligned}
u_k^{\rm ip} &= \exp(\tfrac{h}{2}\mathcal{D})u_k \\
\alpha_1 &= \exp(\tfrac{h}{2}\mathcal{D})\mathcal{N}(u_k), \quad \alpha_2 = \mathcal{N}(u_k^{\rm ip} + \tfrac{h}{2}\alpha_1), \quad \alpha_3 = \mathcal{N}(u_k^{\rm ip} + \tfrac{h}{2}\alpha_2), \\
\alpha_4' &= \mathcal{N}(\exp(\tfrac{h}{2}\mathcal{D})[u_k^{\rm ip} + h\alpha_3])
\end{aligned} \tag{2.12}$$

and

$$u_{k+1} = \exp(\tfrac{h}{2}\mathcal{D})\big(u_k^{\mathrm{ip}} + \tfrac{h}{6}\left(\alpha_1 + 2\alpha_2 + 2\alpha_3\right)\big) + \tfrac{h}{6}\alpha_4'. \tag{2.13}$$

Compared to the computational scheme (2.10)–(2.11), the new formulation saves one evaluation of $\exp(-\frac{h}{2}\mathcal{D})$. Of course the key-point in the computational procedure (2.12)–(2.13) lies in the way the linear operator $\exp(\frac{h}{2}\mathcal{D})$ and nonlinear operator $\mathcal{N}$ are computed.

2.2.2. Computing the $\exp(\frac{h}{2}\mathcal{D})$ terms. For a given $f \in \mathbb{H}^m(\mathbb{R},\mathbb{C})$, we want to compute numerically terms of the form: $\exp(\frac{h}{2}\mathcal{D})f$. In other words, we have to solve the linear PDE problem:

$$\frac{\partial}{\partial z}v(z) = \mathcal{D}v(z) \qquad \forall z \in [z_k, z_{k+1}], \qquad v(z_k) = f. \tag{2.14}$$

The solution to problem (2.14) can be computed by using the Fourier Transform (FT) approach. For a fixed value of the space variable z, we introduce the FT $\widehat{v}(z)$ of $v(z)$ with respect to the time variable t. We denote by $\mathcal{F}$ the Fourier operator from $\mathbb{L}^2(\mathbb{R},\mathbb{C})$ to $\mathbb{L}^2(\mathbb{R},\mathbb{C})$ defined by continuous extension of

$$\forall \psi \in \mathbb{L}^1(\mathbb{R}) \cap \mathbb{L}^2(\mathbb{R}), \quad \forall \nu \in \mathbb{R}, \qquad \mathcal{F}(\psi)(\nu) = \widehat{\psi}(\nu) = \int_{\mathbb{R}} \psi(t)\, \mathrm{e}^{2\mathrm{i}\pi\nu t}\, \mathrm{d}t.$$

From (2.14) we deduce that $\widehat{v}$ satisfies

$$\frac{\mathrm{d}}{\mathrm{d}z}\widehat{v}(z) = \widehat{\mathcal{D}_\nu}\,\widehat{v}(z) \qquad \forall z \in [z_k, z_{k+1}], \qquad \widehat{v}(z_k) = \widehat{f}, \tag{2.15}$$

where $\widehat{\mathcal{D}_\nu} : w \in \mathbb{L}^2(\mathbb{R},\mathbb{C}) \mapsto \sum_{n=2}^{N} \beta_n \frac{\mathrm{i}^{n+1}}{n!}(-2\mathrm{i}\pi\nu)^n w$. Hence

$$\widehat{v}(z) = \widehat{f}\, \mathrm{e}^{\widehat{d}_\nu (z - z_k)} \quad \text{where} \quad \widehat{d}_\nu = \mathrm{i}\sum_{n=2}^{N} \frac{\beta_n}{n!}(2\pi\nu)^n. \tag{2.16}$$

From (2.16) we deduce that

$$\exp(\tfrac{h}{2}\mathcal{D})f = v(z_k + \tfrac{h}{2}) = \mathcal{F}^{-1}\big[\widehat{f}\, \mathrm{e}^{\widehat{d}_\nu \frac{h}{2}}\big] \tag{2.17}$$

where $\mathcal{F}^{-1}$ denotes the inverse Fourier Transform operator.

The following lemma provides a first order Taylor expansion of $\exp(\frac{h}{2}\mathcal{D})f$ for small h and it will be useful later on when the accuracy of the RK4-IP method will be investigated.

LEMMA 2.1. *Let $f \in \mathbb{H}^{N+1}(\mathbb{R},\mathbb{C})$; for $h \in \mathbb{R}_+^*$ in a neighbourhood of 0 we have the following equalities in $\mathbb{H}^1(\mathbb{R},\mathbb{C})$: $\exp(\pm\frac{h}{2}\mathcal{D})f = f \pm \frac{h}{2}\mathcal{D}f + o(h)$. Moreover, when $f \in \mathbb{H}^{2N+1}(\mathbb{R},\mathbb{C})$ we have*

$$\exp(\pm\tfrac{h}{2}\mathcal{D})f = f \pm \frac{h}{2}\mathcal{D}f + \mathcal{O}(h^2). \tag{2.18}$$

2.2.3. Computing the nonlinear terms. When the numerical scheme (2.12)–(2.13) is applied for solving the GNLSE (1.1) one needs to compute for various mappings $f : (z,t) \in [0,L]\times\mathbb{R} \mapsto f(z,t) \in \mathbb{C}$ the nonlinear terms

$$\mathcal{N}(f)(z) = -\frac{\alpha}{2}f(z) + \mathrm{i}\gamma\left(\mathrm{I_d} + \frac{1}{\omega_0}\frac{\partial}{\partial t}\right)\Big[f(z)\big((1-f_R)|f(z)|^2 + f_R\, h_R \star |f(z)|^2\big)\Big] \tag{2.19}$$

where $\star$ denotes the convolution product. One way of computing this quantity is by means of the Fourier Transform. Indeed, time derivation of functions coincides with multiplying the FT of the function by a factor $-2\mathrm{i}\pi\nu$. Namely,

$$\forall \nu \in \mathbb{R} \qquad \big(\widehat{\mathcal{N}}(f)(z)\big)(\nu) = -\frac{\alpha}{2}\mathcal{F}\big(f(z)\big)(\nu) + \mathrm{i}\gamma\left(1 - \frac{2\mathrm{i}\pi\nu}{\omega_0}\right)\times \mathcal{F}\Big[f(z)\big((1-f_R)|f(z)|^2 + f_R\, h_R \star |f(z)|^2\big)\Big](\nu)$$

where we denote by $\widehat{\mathcal{N}}(f)$ the FT of $\mathcal{N}(f)$, for f in the domain of $\mathcal{N}$. Furthermore, to compute the convolution product we can use to the properties of the FT with respect to convolution as follows: $h_R \star |f(z)|^2 = \mathcal{F}^{-1}[\mathcal{F}(h_R) \times \mathcal{F}(|f(z)|^2)]$.

2.2.4. The RK4-IP algorithm for solving the GNLSE. The computation of the 4 terms involving the $\exp(\frac{h}{2}\mathcal{D})$ operator in the computational procedure (2.12)–(2.13) entails the use of the Fourier and Inverse Fourier Transforms. In order to reduce the number of FT to achieve we recast the computational procedure.

Taking into account relation (2.17) we compute at step k for $k = 0, \ldots, K-1$:

$$\begin{aligned}
&\widehat{u}_k^{\mathrm{ip}} = \mathrm{e}^{\widehat{d_\nu}\frac{h}{2}} \times \widehat{u}_k \\
&\widehat{\alpha}_1 = \mathrm{e}^{\widehat{d_\nu}\frac{h}{2}} \times \widehat{\mathcal{N}}(u_k), \quad \widehat{\alpha}_2 = \widehat{\mathcal{N}}\big(\mathcal{F}^{-1}(\widehat{u}_k^{\mathrm{ip}} + \tfrac{h}{2}\widehat{\alpha}_1)\big), \quad \widehat{\alpha}_3 = \widehat{\mathcal{N}}\big(\mathcal{F}^{-1}(\widehat{u}_k^{\mathrm{ip}} + \tfrac{h}{2}\widehat{\alpha}_2)\big) \\
&\widehat{\alpha}_4' = \widehat{\mathcal{N}}\big(\mathcal{F}^{-1}(\mathrm{e}^{\widehat{d_\nu}\frac{h}{2}} \times [\widehat{u}_k^{\mathrm{ip}} + h\widehat{\alpha}_3])\big)
\end{aligned} \tag{2.20}$$

where d_ν is defined in (2.16), and

$$\begin{aligned}
&\widehat{u}_{k+1} = \mathrm{e}^{\widehat{d_\nu}\frac{h}{2}} \times \big(\widehat{u}_k^{\mathrm{ip}} + \tfrac{h}{6}\left(\widehat{\alpha}_1 + 2\widehat{\alpha}_2 + 2\widehat{\alpha}_3\right)\big) + \tfrac{h}{6}\widehat{\alpha}_4' \\
&u_{k+1} = \mathcal{F}^{-1}\big(\widehat{u}_{k+1}\big)
\end{aligned} \tag{2.21}$$

The algorithm for solving the PDE problem (1.8) with $\mathcal{N}$ defined by (2.19) by the RK4-IP method is given in Appendix B. The number of FT per step is 16.

2.2.5. Some important remarks. An important point to be mentioned about the RK4-IP method concerns the values of the *elementary quadrature nodes* $c_1 = 0$, $c_2 = \frac{1}{2}$, $c_3 = \frac{1}{2}$ and $c_4 = 1$ in the classical 4th order RK formula for the efficiency of the RK4-IP method. Indeed, in conjunction with the choice of $z_{k+\frac{1}{2}} = z_k + \frac{h}{2}$ in the change of unknown (2.2), these particular values for the c_i coefficients enable the cancellation of 4 exponential operator terms in (2.10) compared to other possible sets of values, and therefore save up computation. As well, any other value z' in the set $]z_k, z_{k+1}[$ could have been chosen rather than the particular value $z_{k+\frac{1}{2}}$ in the change of unknown (2.2); however the benefit of the cancellation of 4 exponential operator terms in (2.10) would have been lost. An embedded Runge-Kutta scheme for the IP method preserving these nice features has been proposed in [3].

A more immediate way of exploiting the Interaction Picture ideas would be to use a change of unknown similar to the one given by (2.2) but for the original problem (1.8). We mean by this to use a unique new unknown on the whole interval $[0, L]$ rather than using various change of unknowns on each of the subintervals $[z_k, z_{k+1}]$. The only difference between these 2 approaches, corresponding respectively to a local and a global change of unknown, lies in the way the subdivision of interval $[0, L]$ is introduced. In the first approach it is used upstream of the RK4 scheme to set an equivalent sequence of linked problems whereas in the second one it is inherent to the RK4 discretisation. The advantage of using the local change of unknown lies in the numerical evaluation of the $\exp(-(z-z')\mathcal{D})$ operator. We have seen that

the $\exp(\frac{h}{2}\mathcal{D})$ operator can be efficiently computed by use of FT and that some cancellations happen reducing the number of terms to be evaluated. It would not be the case with the second approach where we would have to compute the operator $\exp(-(z_{k+1}-z')\mathcal{D})$ for all $k \in \{0,\dots,K-1\}$.

2.3. Error analysis of the Interaction Picture method. In this section, we proceed to the mathematical analysis of the IP method. Hence, we only consider here the simplified version (1.2) of the GNLSE (1.1). In other terms, we take $\omega_0 = +\infty$ and $f_R = 0$ and then the nonlinearity $\mathcal{N}$ is reduced to $\mathcal{N}_0$.

From Lemmas 1.2 and 1.3, we deduce the following result on the mapping $\mathcal{G}_k$ defined by

$$\begin{array}{rcl} \mathcal{G}_k : [z_k, z_{k+1}] \times \mathbb{H}^1(\mathbb{R},\mathbb{C}) & \longrightarrow & \mathbb{H}^1(\mathbb{R},\mathbb{C}) \\ (z, v) & \longmapsto & \exp(-(z-z_{k+\frac{1}{2}})\mathcal{D}) \left[\mathcal{N}_0\left(\exp((z-z_{k+\frac{1}{2}})\mathcal{D})v\right)\right]. \end{array} \tag{2.22}$$

LEMMA 2.2. *Let $\omega_0 = +\infty$, $f_R = 0$. Then, for all $m \geq 1$, the function $z \mapsto \mathcal{G}_k(z, v(z))$ belongs to $E_{m,N}([z_k, z_{k+1}])$ whenever $v \in E_{m,N}([z_k, z_{k+1}])$. Moreover, for all $M > 0$, there exists $\widetilde{\Lambda}_M > 0$ such that*

$$\forall u, v \in B_M = \{w \in \mathbb{H}^1(\mathbb{R},\mathbb{C}) \,:\, \|w\|_1 \leq M\},$$

we have the estimate: $\|\mathcal{G}_k(u) - \mathcal{G}_k(v)\|_1 \leq \widetilde{\Lambda}_M \, \|u - v\|_1$.

Let $a_0 \in \mathbb{H}^m(\mathbb{R},\mathbb{C})$ with $m \geq 4N+1$ and let us fix once for all the finite integration interval $[0, L]$ such that $0 < L < Z$, where Z is defined in Theorem 1.1 (recall that, if N is even, then we have $Z = +\infty$ and then any $L > 0$ is allowed). Considering the unique solution $A(z)$ of (1.2) given by Theorem 1.1, we have $A \in E_{m,N}([0, L])$, and in particular we have the bound

$$M := \max_{z\in[0,L]} \|A(z)\|_1 < +\infty. \tag{2.23}$$

Denoting $a_k = A(z_k)$ as in Section 2.1, we have then $\|a_k\|_1 \leq M$ for all $0 \leq k \leq K = L/h$. From Theorem 1.1 and Lemma 2.2 one can deduce that problems (2.1) and (2.4) are equivalent. Namely, since $a_k \in \mathbb{H}^m(\mathbb{R},\mathbb{C})$, each one of the 2 problems has a unique solution belonging to $E_{m,N}([z_k, z_{k+1}])$ and the solutions are related to each other through relation (2.2). However, one can also deduce from Lemma 2.2 that A_k^{ip} is slightly more regular than A_k in the sense that $A_k \in E_{m,N}([z_k, z_{k+1}])$, whereas we have

$$A_k^{\mathrm{ip}} \in \bigcap_{j=0}^{\lfloor m/N \rfloor} \mathcal{C}^{j+1}([0, L], \mathbb{H}^{m-Nj}([z_k, z_{k+1}],\mathbb{C})), \tag{2.24}$$

with uniformly bounded norms (i.e. independent of h).

The transformation of the initial problem (1.9) into the three nested problems (2.6)–(2.7)–(2.8) does not imply approximation. As mentioned earlier, problems (2.6) and (2.8) are solved by means of Fourier Transforms (FT) and the numerical accuracy of the computations is the one of the Fast Fourier Transform (FFT) algorithm for evaluating continuous FT of functions [2, 14]. Problem (2.7) is the only one solved using an approximation scheme and therefore (up to the very small spectral error of the FFT) the error in the IP method is essentially the approximation error when solving this ODE problem by the 4th order Runge-Kutta method, with t as a parameter. Therefore, the approximation error in the RK4-IP method at grid point z_{k+1} (neglecting the FFT computational error) is given by

$$e_{k+1} = A(z_{k+1}) - u_{k+1} = \exp(\tfrac{h}{2}\mathcal{D})(A_k^{\mathrm{ip}}(z_{k+1}) - u_{k+1}^{\mathrm{ip}}) \tag{2.25}$$

where u_{k+1}^{ip} denotes the approximate solution to problem (2.7) computed at grid point z_{k+1} by one step of the RK4 method following the approximation scheme (2.9)–(2.10). Thus, the difference $A_k^{\mathrm{ip}}(z_{k+1}) - u_{k+1}^{\mathrm{ip}}$ for one step of the RK4-IP method coincides with the local error ℓ_k of the RK4 method defined by

$$A_k^{\mathrm{ip}}(z_{k+1}) = A_k^{\mathrm{ip}}(z_k) + h\,\Phi(z_k, A_k^{\mathrm{ip}}(z_k); h) + \ell_k. \tag{2.26}$$

For the standard RK4 method, provided all the partial derivatives of $(z, A) \mapsto \mathcal{G}_k(z, A)$ exist and are continuous up to the order 5, the local error ℓ_k is known to behave as $\ell_k = \mathcal{O}(h^5)$ [5, 18, 10]. From (2.24), we infer that, since we have assumed that $m \geq 4N + 1$, the z-derivatives of $\mathcal{G}_k(z, A_k^{\mathrm{ip}})$ up to the order 5 are uniformly bounded in $\mathbb{H}^1(\mathbb{R}, \mathbb{C})$. This means that we have for the local error the following estimate

$$\forall k \in \{0, \ldots, K\} \qquad \|\ell_k\|_1 \leq Ch^5 \tag{2.27}$$

where $C > 0$ is independent of h.

In order to estimate the global error for the RK4-IP method, we first need a Lipschitz estimate for the increment function Φ.

LEMMA 2.3. *Let $\omega_0 = +\infty$, $f_R = 0$, let $M > 0$ and let $\Lambda = \widetilde{\Lambda}_M$ be the Lipschitz constant for $\mathcal{G}_k$ given by Lemma 2.2. Then the increment function Φ defined in* (2.10) *satisfies the following Lipschitz condition: $\forall A, B \in B_M$,*

$$\|\Phi(z, A; h) - \Phi(z, B; h)\|_1 \leq \Lambda\big(1 + \tfrac{1}{2}h\Lambda + \tfrac{1}{6}h^2\Lambda^2 + \tfrac{1}{24}h^3\Lambda^3\big)\,\|A - B\|_1.$$

Proof. On the one hand, from the expression of the increment function Φ given by (2.10), we have: $\forall z \in [0, L]$, $\forall A, B \in B_M$,

$$\Phi(z, A; h) - \Phi(z, B; h) = \frac{1}{6}(\alpha_1^A - \alpha_1^B) + \frac{1}{3}(\alpha_2^A - \alpha_2^B) + \frac{1}{3}(\alpha_3^A - \alpha_3^B) + \frac{1}{6}(\alpha_4^A - \alpha_4^B) \tag{2.28}$$

where α_j^A (resp. α_j^B), $j \in \{1, \ldots, 4\}$ stands for $\alpha_j(z_k, A; h)$ (resp. $\alpha_j(z_k, B; h)$). On the other hand, from the Lipschitz condition satisfied by $\mathcal{G}_k$ we deduce the following inequalities: $\forall z \in [0, L]$, $\forall A, B \in B_M$

$$\begin{aligned}
\|\alpha_1^A - \alpha_1^B\|_1 &= \|\mathcal{G}_k(z, A) - \mathcal{G}_k(z, B)\|_1 \leq \Lambda\|A - B\|_1\,, \\
\|\alpha_2^A - \alpha_2^B\|_1 &= \|\mathcal{G}_k(z + \tfrac{h}{2}, A + \tfrac{h}{2}\alpha_1^A) - \mathcal{G}_k(z + \tfrac{h}{2}, B + \tfrac{h}{2}\alpha_1^B)\|_1 \\
&\leq \Lambda\|A - B + \tfrac{h}{2}(\alpha_1^A - \alpha_1^B)\|_1 \leq \Lambda(1 + \tfrac{h\Lambda}{2})\,\|A - B\|_1.
\end{aligned}$$

In the same way we obtain

$$\begin{aligned}
\|\alpha_3^A - \alpha_3^B\|_1 &\leq \Lambda(1 + \tfrac{h\Lambda}{2} + \tfrac{h^2\Lambda^2}{4})\,\|A - B\|_1\,, \\
\|\alpha_4^A - \alpha_4^B\|_1 &\leq \Lambda(1 + \tfrac{h\Lambda}{2} + \tfrac{h^2\Lambda^2}{2} + \tfrac{h^3\Lambda^3}{4})\,\|A - B\|_1.
\end{aligned}$$

Applying the triangle inequality to (2.28) and using the above inequalities we obtain the result. □

We also need the following version of the discrete Gronwall's lemma (its proof is straightforward by mathematical induction).

LEMMA 2.4. *Let $(\theta_k)_{k\in\mathbb{N}}$ and $(\varepsilon_k)_{k\in\mathbb{N}}$ be two non-negative sequences of real numbers and let h and λ be two non-negative real numbers such that*

$$\theta_{k+1} \leq (1 + h\lambda)\theta_k + \varepsilon_k,\ \forall k \in \mathbb{N}.$$

Then, for all $k \in \mathbb{N}^*$,

$$\theta_k \leq \mathrm{e}^{kh\lambda}\,\theta_0 + \sum_{j=0}^{k-1} \mathrm{e}^{(k-1-j)h\lambda}\varepsilon_j.$$

We are now in position to prove our main result concerning the error analysis in the RK4-IP method.

THEOREM 2.5. *Let* $a_0 \in \mathbb{H}^{4N+1}(\mathbb{R},\mathbb{C})$, *let* $A \in E_{m,N}([0,Z[)$ *be the maximal solution to* (1.2) *given by Theorem 1.1 and let* $0 < L < Z$. *Consider a constant step-size subdivision of interval* $[0,L]$ *into* K *subintervals by the points* $z_0,\ldots,z_K$ *arranged in increasing order. Let us denote by* A *the solution of* (1.9) *(equivalently, of* (1.2)*) and by* $(u_k)_{k=0\ldots,K}$ *the sequence defined by* (2.20)-(2.21). *Then there exists* $C > 0$ *such that*

$$\max_{k=0,\ldots,K} \|A(z_k) - u_k\|_1 \leq CLh^4. \tag{2.29}$$

Proof. In this proof, we systematically assume that the numerical solution u_k defined by the algorithm (2.20)-(2.21) satisfies the bound $\|u_k\|_1 \leq 2M$ for all $0 \leq k \leq K$. In fact, this bound can be a posteriori checked, for h small enough, thanks to (2.23) and the final estimate (2.29). Hence, with the notation of Lemma 2.2, we always have

$$\forall k \in \{0,\ldots,K\} \qquad A_k(z_k) \in B_{2M} \quad \text{and} \quad u_k \in B_{2M}. \tag{2.30}$$

When the RK4-IP method is applied for solving problem (1.9) the global error at grid point z_{k+1} is given by (2.25) and from (2.9) and (2.26) we have

$$\begin{aligned} A_k^{\mathrm{ip}}(z_{k+1}) &= \exp(\tfrac{h}{2}\mathcal{D})A_k(z_k) + h\,\Phi(z_k,\exp(\tfrac{h}{2}\mathcal{D})A_k(z_k);h) + \ell_k \\ u_{k+1}^{\mathrm{ip}} &= \exp(\tfrac{h}{2}\mathcal{D})u_k + h\,\Phi(z_k,\exp(\tfrac{h}{2}\mathcal{D})u_k;h) \end{aligned}$$

so that

$$\begin{aligned} e_{k+1} = {}& \exp(h\mathcal{D})[A_k(z_k) - u_k] + h\exp(\tfrac{h}{2}\mathcal{D})\big[\Phi(z_k,\exp(\tfrac{h}{2}\mathcal{D})A_k(z_k);h) \\ & - \Phi(z_k,\exp(\tfrac{h}{2}\mathcal{D})u_k;h)\big] + \exp(\tfrac{h}{2}\mathcal{D})\ell_k. \end{aligned} \tag{2.31}$$

Since Φ satisfies the Lipschitz condition of Lemma 2.3, since we have the bounds (2.30) and since $\exp(\frac{h}{2}\mathcal{D})$ is an isometry on $\mathbb{H}^1(\mathbb{R},\mathbb{C})$, we successively have

$$\begin{aligned} \|\Phi(z_k,\exp(\tfrac{h}{2}\mathcal{D})A_k(z_k);h) - \Phi(z_k,\exp(\tfrac{h}{2}\mathcal{D})u_k;h)\|_1 &\leq \widetilde{\Lambda}\,\|\exp(\tfrac{h}{2}\mathcal{D})A_k(z_k) - \exp(\tfrac{h}{2}\mathcal{D})u_k\|_1 \\ &\leq \widetilde{\Lambda}\,\|A_k(z_k) - u_k\|_1 \end{aligned} \tag{2.32}$$

where $\widetilde{\Lambda} = \Lambda(1 + \frac{1}{2}h\Lambda + \frac{1}{6}h^2\Lambda^2 + \frac{1}{24}h^3\Lambda^3)$ and $\Lambda = \widetilde{\Lambda}_{2M}$ (defined in Lemma 2.2). Taking the norm of (2.31), using the triangle inequality and (2.32), yields $\|e_{k+1}\|_1 \leq (1 + h\widetilde{\Lambda})\,\|e_k\|_1 + \|\ell_k\|_1$. From Lemma 2.4, we deduce that for all $k \in \{0,\ldots,K-1\}$

$$\|e_k\|_1 \leq \mathrm{e}^{kh\widetilde{\Lambda}}\,\|e_0\|_1 + \sum_{j=0}^{k-1} \mathrm{e}^{(k-1-j)h\widetilde{\Lambda}}\|\ell_j\|_0 \leq \mathrm{e}^{L\widetilde{\Lambda}}\,\big(\|e_0\|_1 + \sum_{j=0}^{k-1}\|\ell_j\|_1\big).$$

Finally, from the error bound (2.27) for the local error we conclude that

$$\max_{k\in\{0,\ldots,K-1\}} \|e_k\|_1 \leq \mathrm{e}^{L\widetilde{\Lambda}}\,\big(\|e_0\|_1 + CLh^4\big).$$

When we assume that the initial data is not perturbed, we have

$$\max_{k\in\{0,\dots,K-1\}} \|A(z_k) - u_k\|_1 \leq \mathrm{e}^{L\widetilde{\Lambda}} CLh^4. \quad \square$$

Remark 2. In Theorem 2.5 we have assumed that all the evaluations of the nonlinear operator $\mathcal{N}_0$ and linear exponential operator $\exp(\frac{h}{2}\mathcal{D})$ were achieved without numerical error by use of the Fourier Transform (FT). Since FT of functions are computed using the Fast Fourier Transform (FFT) algorithm, there is an additional error in the RK4-IP method. We refer to [2, 14] for an analysis of the error when the continuous FT of functions is evaluated by the FFT algorithm. When evaluating FT by the FFT algorithm, once the size T of the time interval and the number m of discretisation points are set, the size of the frequency interval is given by the Nyquist frequency $\nu_N = m/T$ and the sampling step-size is $h_\nu = 1/T$. One practical consequence when dealing with problems in nonlinear optics is that the number of discretisation points m has usually to be chosen very large in order to have a frequency window wide enough to embrace all the physical relevant information (e.g. the study of pulsed laser systems with fiber amplifier described in [15] imposes values of m in the range 2^{20}–2^{23}). Therefore, although there exists an additional error in the RK4-IP method related to the computation of FT, this error is generally several orders of magnitude lower than the approximation error in the RK4-IP method.

3. Comparison of IP and Symmetric Split-Step methods. As shown in Section 2, the RK4-IP method is based on the change of unknown given by relation (2.2) leading to a set of three nested PDE problems (2.6)–(2.7)–(2.8) to be solved over each subinterval introduced with the discretisation of the fiber length. This computational structure is very similar to what is obtained when solving problem (1.8) by the Split-Step method based on the Strang splitting formula [29] also termed Symmetric Split-Step (S3) method.

3.1. Solving the GNLSE by the Symmetric Split-Step (S3) method. Here again the interval $[0, L]$ is divided into K subintervals where the spatial grid points are denoted z_k, $k \in \{0, \dots, K\}$, where $0 = z_0 < z_1 < \cdots < z_{K-1} < z_K = L$. For convenience we assume a constant grid spacing $h = L/K$ but this assumption is not a limitation of the method and we set $z_{k+\frac{1}{2}} = z_k + \frac{h}{2}$. The S3 method consists in solving over each subinterval $[z_k, z_{k+1}]$ for $k \in \{0, \dots, K-1\}$, the following three nested problems with time variable t as a parameter:

$$\frac{\partial}{\partial z} A_k^+(z) = \mathcal{D} A_k^+(z) \quad \forall z \in [z_k, z_{k+\frac{1}{2}}], \qquad A_k^+(z_k) = A_{k-1}(z_k), \tag{3.1}$$

where $A_{k-1}(z_k)$ represents the approximate solution at grid point z_k computed at step $k-1$;

$$\frac{\partial}{\partial z} B_k(z) = \mathcal{N}(B_k)(z) \quad \forall z \in [z_k, z_{k+1}], \qquad B_k(z_k) = A_k^+(z_{k+\frac{1}{2}}), \tag{3.2}$$

where $A_k^+(z_{k+\frac{1}{2}}, t)$ represents the solution to problem (3.1) at half grid point $z_{k+\frac{1}{2}}$;

$$\frac{\partial}{\partial z} A_k^-(z) = \mathcal{D} A_k^-(z) \quad \forall z \in [z_{k+\frac{1}{2}}, z_{k+1}], \qquad A_k^-(z_{k+\frac{1}{2}}) = B_k(z_{k+1}), \tag{3.3}$$

where $B_k(z_{k+1}, t)$ represents the solution to problem (3.2) at node z_{k+1}. An approximate solution to problem (1.8) at grid node z_{k+1} is then given by $A_k(z_{k+1}) := A_k^-(z_{k+1})$.

The solutions to problems (3.1) and (3.3) at grid points $z_{k+\frac{1}{2}}$ and z_{k+1} respectively can be expressed as

$$A_k^+(z_{k+\frac{1}{2}}) = \exp(\tfrac{h}{2}\mathcal{D}) A_{k-1}(z_k)$$

and

$$A_k^-(z_{k+1}) = \exp(\tfrac{h}{2}\mathcal{D})B_k(z_{k+1}).$$

The two linear PDE problems (3.1) and (3.3) are solved according to the computational procedure outlined in Section 2.2.2 by means of the Fourier Transform. The solution to the nonlinear ODE problem (3.2) can be approximated using usual numerical schemes for ODE and the choice of the classical RK4 method is usual. One step of the RK4 scheme applied to problem (3.2) reads:

$$B_k(z_{k+1}) \approx u_{k+1} = B_k(z_k) + \frac{h}{6}\left(\alpha_1 + 2\alpha_2 + 2\alpha_3 + \alpha_4\right), \tag{3.4}$$

$\alpha_1 = \mathcal{N}(B_k(z_k)),\ \alpha_2 = \mathcal{N}(B_k(z_k) + \frac{h}{2}\alpha_1),\ \alpha_3 = \mathcal{N}(B_k(z_k) + \frac{h}{2}\alpha_2),\ \alpha_4 = \mathcal{N}(B_k(z_k) + h\alpha_3).$

As the numerical resolution of the linear PDE problems (3.1) and (3.3) as well as the evaluation of the nonlinear terms involve the use of the Fourier and Inverse Fourier Transforms, here again it is convenient to recast the computational procedure in order to reduce the number of FT to achieve. We make use of the notations introduced in Section 2.2.4. Taking into account relation (2.17), we transform the computational sequence (3.4) in the following way: at step k for $k = 0, \ldots, K-1$ we compute

$$\begin{aligned}
&\widehat{u}_{k+\frac{1}{2}} = \mathrm{e}^{\widehat{d}_\nu \frac{h}{2}}\widehat{u}_k \\
&\widehat{\alpha}_1 = \widehat{\mathcal{N}}(\mathcal{F}^{-1}(\widehat{u}_{k+\frac{1}{2}})), && \widehat{\alpha}_2 = \widehat{\mathcal{N}}\big(\mathcal{F}^{-1}(\widehat{u}_{k+\frac{1}{2}} + \tfrac{h}{2}\widehat{\alpha}_1)\big) \\
&\widehat{\alpha}_3 = \widehat{\mathcal{N}}\big(\mathcal{F}^{-1}(\widehat{u}_{k+\frac{1}{2}} + \tfrac{h}{2}\widehat{\alpha}_2)\big), && \widehat{\alpha}_4 = \widehat{\mathcal{N}}\big(\mathcal{F}^{-1}(\widehat{u}_{k+\frac{1}{2}} + h\widehat{\alpha}_3)\big)
\end{aligned}$$

and

$$\widehat{u}_{k+1} = \mathrm{e}^{\widehat{d}_\nu \frac{h}{2}} \times \big(\widehat{u}_{k+\frac{1}{2}} + \tfrac{h}{6}\left(\widehat{\alpha}_1 + 2\widehat{\alpha}_2 + 2\widehat{\alpha}_3 + \widehat{\alpha}_4\right)\big), \qquad u_{k+1} = \mathcal{F}^{-1}\big(\widehat{u}_{k+1}\big).$$

The above computational scheme is referred to as the Symmetric Split-Step Fourier with 4th order Runge-Kutta formula (S3F-RK4) method. It has to be compared to the computational scheme (2.20)–(2.21) for solving the GNLSE (1.1) by the RK4-IP method. The algorithm for solving the GNLSE by the S3F-RK4 method is given in Appendix C. It involves 16 FFT per step.

3.2. Theoretical comparison of Interaction Picture method and Symmetric Split-Step method. Again, in this section, we assume that $\omega_0 = +\infty$ and that $f_R = 0$. From our presentation of both the RK4-IP and S3F-RK4 methods, a formal comparison of the two methods is straightforward. Over one subinterval $[z_k, z_{k+1}]$ the three nested problems (2.6) – (2.7) – (2.8) are solved when the RK4-IP method is used whereas with the S3F-RK4 method the three nested problems (3.1) – (3.2) – (3.3) are solved. Since problems (2.6) and (3.1) are the same as well as problems (2.8) and (3.3), the difference between the two computational methods lies in problems (2.7) and (3.2). Both are solved here using the same 4th order Runge-Kutta method. The splitting (2.6) – (2.7) – (2.8) is exact since it originates from the change of unknown (2.2) whereas the splitting (3.1) – (3.2) – (3.3) deduced from the Strang formula is second-order accurate. To be comprehensive, we have the following relationship between the solution to problems (2.7) and (3.2).

PROPOSITION 3.1. *Let $\omega_0 = +\infty$, $f_R = 0$. For all $k \in \{0, \ldots, K-1\}$ let B_k denote the solution to problem* (3.2) *and A_k^{ip} denote the solution to problem* (2.7) *with the same initial data $A_k^+(z_{k+\frac{1}{2}})$ assumed to belong to $\mathbb{H}^{3N+1}(\mathbb{R},\mathbb{C})$. Then, for all $k \in \{0, \ldots, K-1\}$ we have the following estimate in $\mathbb{H}^1(\mathbb{R},\mathbb{C})$:*

$$B_k(z_{k+1}) = A_k^{\mathrm{ip}}(z_{k+1}) + \mathcal{O}(h^3).$$

Proof. We first consider the second order Taylor expansion of the solution to problems (3.2) and (2.7) in z_k with respect to the first variable z (as before, the second variable t is omitted and equalities hold in $\mathbb{H}^1(\mathbb{R},\mathbb{C})$):

$$A_k^{\mathrm{ip}}(z_{k+1}) = A_k^{\mathrm{ip}}(z_k) + h\,\partial_1 A_k^{\mathrm{ip}}(z_k) + \frac{h^2}{2}\,\partial_{11}^2 A_k^{\mathrm{ip}}(z_k) + \mathcal{O}(h^3)$$
$$B_k(z_{k+1}) = B_k(z_k) + h\,\partial_1 B_k(z_k) + \frac{h^2}{2}\,\partial_{11}^2 B_k(z_k) + \mathcal{O}(h^3).$$

Since the initial condition in (3.2) and (2.7) are identical, by difference we obtain

$$\begin{aligned} A_k^{\mathrm{ip}}(z_{k+1}) - B_k(z_{k+1}) =& h\Big(\partial_1 A_k^{\mathrm{ip}}(z_k) - \partial_1 B_k(z_k)\Big) \\ &+ \frac{h^2}{2}\Big(\partial_{11}^2 A_k^{\mathrm{ip}}(z_k) - \partial_{11}^2 B_k(z_k)\Big) + \mathcal{O}(h^3). \end{aligned} \tag{3.5}$$

From the PDE in (3.2) and (2.7) we have $\partial_1 B_k(z_k) = \mathcal{N}_0(B_k)(z_k) = \mathcal{N}_0(A_k^+)(z_{k+\frac12})$ and

$$\begin{aligned} \partial_1 A_k^{\mathrm{ip}}(z_k) &= \mathcal{G}_k(z_k, A_k^{\mathrm{ip}}) = \exp(\tfrac{h}{2}\mathcal{D})\mathcal{N}_0\big(\exp(-\tfrac{h}{2}\mathcal{D})A_k^{\mathrm{ip}}\big)(z_k) \\ &= \exp(\tfrac{h}{2}\mathcal{D})\mathcal{N}_0\big(\exp(-\tfrac{h}{2}\mathcal{D})A_k^{+}\big)(z_{k+\frac12}) \\ &= \mathcal{N}_0\big(\exp(-\tfrac{h}{2}\mathcal{D})A_k^{+}\big)(z_{k+\frac12}) + \frac{h}{2}\mathcal{D}\mathcal{N}_0\big(\exp(-\tfrac{h}{2}\mathcal{D})A_k^{+}\big)(z_{k+\frac12}) + \mathcal{O}(h^2) \end{aligned} \tag{3.6}$$

where the last relation results from the expansion given in Lemma 2.1. Now consider a Taylor expansion of the operator $\mathcal{N}_0$ between $v_k = A_k^+(z_{k+\frac12})$ and $w_k = \exp(-\frac{h}{2}\mathcal{D})A_k^+(z_{k+\frac12})$:

$$\mathcal{N}_0(w_k) = \mathcal{N}_0(v_k) + \mathcal{N}_0'(v_k)(w_k - v_k) + \mathcal{O}\big(\|w_k - v_k\|_1^2\big). \tag{3.7}$$

From Lemma 2.1 considered with $A_k^+(z_{k+\frac12})$ we obtain

$$w_k - v_k = \exp(-\tfrac{h}{2}\mathcal{D})A_k^+(z_{k+\frac12}) - A_k^+(z_{k+\frac12}) = -\frac{h}{2}\,\mathcal{D}A_k^+(z_{k+\frac12}) + \mathcal{O}(h^2)$$

so that from (3.7)

$$\mathcal{N}_0(w_k) - \mathcal{N}_0(v_k) = \mathcal{N}_0(A_k^+)(z_{k+\frac12}) - \frac12\,\mathcal{D}A_k^+(z_{k+\frac12})\mathcal{N}_0'(A_k^+)(z_{k+\frac12})h + \mathcal{O}\big(h^2\big). \tag{3.8}$$

Finally, from (3.6) and (3.8) we have

$$\begin{aligned} \partial_1 A_k^{\mathrm{ip}}(z_k) = \mathcal{N}_0(A_k^+)(z_{k+\frac12}) &+ \frac{h}{2}\,\mathcal{D}\mathcal{N}_0(A_k^+)(z_{k+\frac12}) \\ &- \frac12\,\mathcal{D}A_k^+(z_{k+\frac12})\mathcal{N}_0'(A_k^+)(z_{k+\frac12})h + \mathcal{O}\big(h^2\big). \end{aligned} \tag{3.9}$$

Now, from (3.5) we obtain

$$\begin{aligned} A_k^{\mathrm{ip}}(z_{k+1}) - B_k(z_{k+1}) = \mathcal{D}\left[\mathcal{N}_0(A_k^+)(z_{k+\frac12}) - A_k^+(z_{k+\frac12})\mathcal{N}_0'(A_k^+)(z_{k+\frac12})\right]\frac{h^2}{2} \\ + \frac{h^2}{2}\Big(\partial_{11}^2 A_k^{\mathrm{ip}}(z_k) - \partial_{11}^2 B_k(z_k)\Big) + \mathcal{O}(h^3). \end{aligned} \tag{3.10}$$

Let us consider in (3.10) the term $\partial_{11}^2 A_k^{\mathrm{ip}}(z_k) - \partial_{11}^2 B_k(z_k)$. On the one hand we have

$$\partial_{11}^2 B_k(z) = \partial_1\big(\partial_1 B_k(z)\big) = \frac{\partial}{\partial z}\mathcal{N}_0(B_k)(z) = \mathcal{N}_0'(B_k)(z)\partial_1 B_k(z)$$

so that for $z = z_k$, using the PDE in (3.2) and then the initial condition we deduce that

$$\begin{aligned}\partial_{11}^2 B_k(z_k) &= \mathcal{N}_0'(B_k)(z_k)\partial_1 B_k(z_k) = \mathcal{N}_0'(B_k)(z_k)\mathcal{N}_0(B_k)(z_k)\\ &= \mathcal{N}_0'(A_k^+)(z_{k+\frac12})\mathcal{N}_0(A_k^+)(z_{k+\frac12}).\end{aligned} \tag{3.11}$$

On the other hand from the PDE in (2.7) we have

$$\begin{aligned}\partial_{11}^2 A_k^{\mathrm{ip}}(z) &= \frac{\partial}{\partial z}\mathcal{G}_k(z, A_k^{\mathrm{ip}}) = \frac{\partial}{\partial z}\Big(\exp(-(z-z_{k+\frac12})\mathcal{D})\mathcal{N}_0\big(\exp((z-z_{k+\frac12})\mathcal{D})A_k^{\mathrm{ip}}\big)\Big)(z)\\ &= -\mathcal{D}\mathcal{G}_k(z,t,A_k^{\mathrm{ip}}) + \mathcal{N}_0'\big(\exp((z-z_{k+\frac12})\mathcal{D})A_k^{\mathrm{ip}}\big)(z)\Big(\mathcal{D}A_k^{\mathrm{ip}}(z) + \partial_1 A_k^{\mathrm{ip}}(z)\Big).\end{aligned}$$

It follows for $z = z_k$ that

$$\partial_{11}^2 A_k^{\mathrm{ip}}(z_k) = -\mathcal{D}\mathcal{G}_k(z_k,t,A_k^{\mathrm{ip}}) + \mathcal{N}_0'\big(\exp(-\tfrac{h}{2}\mathcal{D})A_k^{\mathrm{ip}}\big)(z_k)\Big(\mathcal{D}A_k^{\mathrm{ip}}(z_k) + \partial_1 A_k^{\mathrm{ip}}(z_k)\Big).$$

From (3.6) we have

$$\mathcal{G}_k(z_k,t,A_k^{\mathrm{ip}}) = \partial_1 A_k^{\mathrm{ip}}(z_k) = \mathcal{N}_0(A_k^+)(z_{k+\frac12}) + \mathcal{O}(h)$$

and a Taylor expansion of $\mathcal{N}_0'$ gives

$$\mathcal{N}_0'\big(\exp(-\tfrac{h}{2}\mathcal{D})A_k^{\mathrm{ip}}\big)(z_k) = \mathcal{N}_0'\big(\exp(-\tfrac{h}{2}\mathcal{D})A_k^{+}\big)(z_{k+\frac12}) = \mathcal{N}_0'(A_k^+)(z_{k+\frac12}) + \mathcal{O}(h),$$

so that

$$\begin{aligned}\partial_{11}^2 A_k^{\mathrm{ip}}(z_k) =& \mathcal{D}\Big[\mathcal{N}_0'(A_k^+)(z_{k+\frac12})A_k^+(z_{k+\frac12}) - \mathcal{N}_0(A_k^+)(z_{k+\frac12})\Big]\\ &+ \mathcal{N}_0'(A_k^+)(z_{k+\frac12})\mathcal{N}_0(A_k^+)(z_{k+\frac12}) + \mathcal{O}(h).\end{aligned} \tag{3.12}$$

Therefore from (3.11) and (3.12) we deduce that

$$\partial_{11}^2 A_k^{\mathrm{ip}}(z_k) - \partial_{11}^2 B_k(z_k) = \mathcal{D}\Big[\mathcal{N}_0'(A_k^+)(z_{k+\frac12})A_k^+(z_{k+\frac12}) - \mathcal{N}_0(A_k^+)(z_{k+\frac12})\Big] + \mathcal{O}(h). \tag{3.13}$$

To conclude, from (3.10) and (3.13) we have $A_k^{\mathrm{ip}}(z_{k+1}) - B_k(z_{k+1}) = \mathcal{O}(h^3)$. □

As problems (2.6) and (3.1) are identical as well as problems (2.8) and (3.3) (and assumed to be solved without approximation by the way of Fourier Transform), we deduce from Proposition 3.1 the following corollary.

Corollary 3.2. *Consider a subdivision of interval $[0, L]$ into K subintervals by the points $z_0, \dots, z_K$ arranged in increasing order. For all $k \in \{0, \dots, K-1\}$ denote by A_k the solution to problem* (1.9) *over the subinterval $[z_k, z_{k+1}]$ and denote by B_k the approximation of the solution to problem* (1.9) *over the subinterval $[z_k, z_{k+1}]$ computed by solving the three nested problems* (3.1)–(3.2)–(3.3). *Then*

$$\sup_{k\in\{0,\dots,K-1\}} \|A_k(z_{k+1}) - B_k(z_{k+1})\|_1 = \mathcal{O}(h^2).$$

Remark 3. The convergence of the Split-Step methods applied to various forms of the Schrödinger equation is studied in e.g. [4, 22] where the authors prove that the convergence order of the S3F method is 2. As the change of unknown in the IP method does not imply approximation before discretization, the second order convergence of the S3F method can alternatively be deduced from Corollary 3.2.

3.3. Numerical comparison. In the framework of a project on the numerical simulation of incoherent optical wave propagation in nonlinear fibers [15] we have implemented both the RK4-IP and S3F-RK4 methods for solving the GNLSE (1.1).

3.3.1. Numerical comparison for simulation of wave propagation in optical fibers. We present in this section numerical results on two selected applications in optics: the propagation of optical solitons and the propagation of a picosecond pulse into a single-mode fiber where fiber losses, nonlinear Raman and Kerr effects and high order chromatic dispersion are taken into account. In both cases, we use the RK4-IP and S3F-RK4 methods with a constant step-size and with an adaptive step-size strategy based on the embedded RK4(3) scheme presented in [3].

We first consider the case of the NLSE (1.3) with $\alpha = 0$. When $\beta_2 < 0$, there exists an exact solution known as the optical soliton [1]. Namely, if the source term is given by $a_0 : t \mapsto N_s/(\sqrt{\gamma L_D}\cosh(tN_S/T_0))$ where N_s is the soliton order, T_0 is the pulse half-width and $L_D = -T_0^2/\beta_2$ is the dispersion length, then the solution to the NLSE reads

$$\forall z \in [0, L], \quad \forall t \in \mathbb{R}, \qquad A(z,t) = \frac{N_s}{\sqrt{\gamma L_D}} \frac{\mathrm{e}^{\mathrm{i}zN_s^2/(2L_D)}}{\cosh(tN_s/T_0)}. \tag{3.14}$$

We carry on comparison with a 3rd order soliton ($N_s = 3$). The physical parameters of the numerical experiment are $L = 637.21\,\mathrm{m}$, $\gamma = 4.3\,\mathrm{W}^{-1}\,\mathrm{km}^{-1}$, $\beta_2 = -19.83\,\mathrm{ps}^2\,\mathrm{km}^{-1}$, $T_0 = 2.8365\,\mathrm{ps}$. The number of sampling points for the FFT computations is set to 2^{16}.

Both algorithms are tested on a Intel Core 2 Quad Q6600, with constant step-size or adaptive step-size. The CPU time, quadratic error and number of steps are compared in Table 3.1.

TABLE 3.1

Comparison of the RK4-IP and S3F-RK4 methods for solving the NLSE. When an adaptive step-size strategy is used, the tolerance for the local error is set to 10^{-6}.

method	CPU time	quadratic error	number of steps
RK4-IP adaptive step-size	69 s	$1.12\,10^{-4}$	605
S3F-RK4 adaptive step-size	67 s	$6.34\,10^{-3}$	563
RK4-IP constant step-size	4840 s	$1.41\,10^{-4}$	63722
S3F-RK4 constant step-size	4651 s	$1.40\,10^{-4}$	63722

We now consider the GNLSE (1.1) with the following set of physical parameters : $\omega_0 = 1770\,\mathrm{Thz}$, $\gamma = 4.3\,\mathrm{W}^{-1}\mathrm{km}^{-1}$, $\beta_2 = 19.83\,\mathrm{ps}^2\mathrm{km}^{-1}$, $\beta_3 = 0.031\,\mathrm{ps}^3\mathrm{km}^{-1}$ and $\beta_n = 0$ for $n \geq 4$, $\alpha = 0.046\,\mathrm{km}^{-1}$, $L = 96,77\,\mathrm{m}$, $f_R = 0.245$. An expression for the Raman time response function for silica core fiber is given in [1]. The source term is $a_0 : t \mapsto \sqrt{P_0}\,\mathrm{e}^{-\frac{1}{2}(t/T_0)^2}$ where $T_0 = 2.8365\,\mathrm{ps}$ is the pulse half-width and $P_0 = 100\,\mathrm{W}$ is the pulse peak power. When using the RK4-IP method with an adaptive step-size strategy with a tolerance of $\mathrm{tol} = 10^{-6}$ and an initial step size of $h = 0.1\,\mathrm{m}$, the number of discretisation steps along the fiber is found to be 279 and the computation time is 50 s. With the S3F-RK4 method we obtain similar results, see table 3.2. When the tolerance is set to $\mathrm{tol} = 10^{-9}$ with an initial step size of $h = 0.1\,\mathrm{m}$, the number of step-size with the RK4-IP method with an adaptive step-size strategy is 1545 steps for a computational time of 221 s and again results obtained with the S3F-RK4 method are very similar. These very close results in terms of computational time can be related to the close structure of the two algorithms. For a more complete experimental comparison between the RK4-IP method and Split-Step methods for solving the GNLSE in optics we refer to [20].

TABLE 3.2
Comparison of the RK4-IP and S3F-RK4 methods for solving the GNLSE with adaptive step-size strategy and tolerance for the local error set to 10^{-6} *and* 10^{-9}.

method	CPU time	quadratic norm	number of steps
RK4-IP - tol = 10^{-6}	50 s	23.01885356801830	279
S3F-RK4 - tol = 10^{-6}	45 s	23.01888354663108	279
RK4-IP - tol = 10^{-9}	221 s	23.01888060906444	1545
S3F-RK4 - tol = 10^{-9}	204 s	23.01888063777934	1545

3.3.2. Numerical comparison of convergence rates. In order to illustrate the result of Theorem 2.5 we have solved the GNLSE (1.1) by the RK4-IP and S3F-RK4 methods with constant step-size values divided by 2 from one execution to the other. We have obtained the experimental convergence curves depicted in Figure 3.1. The physical values used for the computation are the one given in the previous section for the GNLSE. This experimental result is in a good agreement with the theoretical convergence behavior predicted by Theorem 2.5 for the RK4-IP method (convergence order 4) and by Corollary 3.2 for the S3F-RK4 method (convergence order 2). We also mention that in other simulations where the nonlinear parameter γ and the power of the source term were larger, we have obtained an experimental convergence order for the S3F-RK4 method close to 4. This can be easily explained as follows: when the "weight" of the nonlinear ODE in Strang splitting (3.1)–(3.2)–(3.3) is much larger than the "weight" of the linear PDE problems (3.1) and (3.3), the error due to the splitting formula (in $\mathcal{O}(h^2)$) can be lower than the error of the RK4 formula (in $\mathcal{O}(h^4)$) which dominates. This explains the observed experimental convergence behavior.

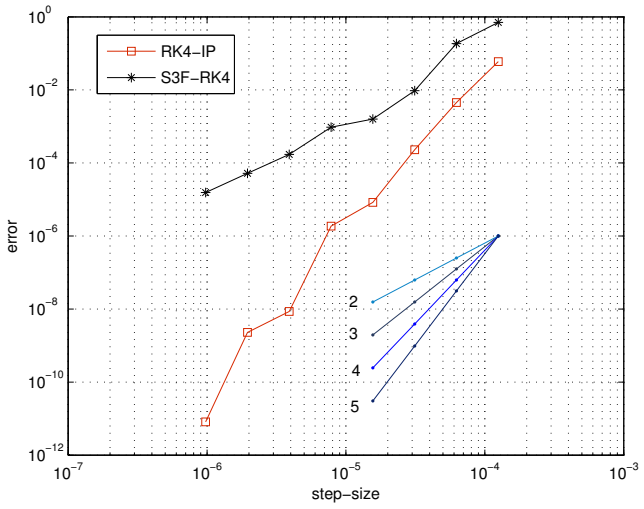

FIG. 3.1. *Experimental convergence curves for the RK4-IP and S3F-RK4 methods.*

4. Conclusion. We have presented an alternative method to the Split-Step approach for solving the GNLSE in optics. The Interaction Picture (IP) method has a form very similar

to the one of the Symmetric Split-Step method. However it is based on a change of unknown rather than on a splitting formula and therefore does not contain any approximation at this stage. Actually, the error in the IP method is in the use of an approximation scheme for solving the nonlinear ODE problem resulting from the change of unknown. We have carried out a theoretical and experimental study of the IP method and we have compared it to the Symmetric Split-Step method. It is worth mentioning that the IP method can be used for a larger number of PDEs than only the GNLSE; actually it is suitable to solve all PDEs where Split-Step methods are generally used.

Appendix A. Proof of Theorem 1.1. In this section, we analyze the well-posedness of the Cauchy problem (1.2) (formulated under the form (1.9)). For simplicity, we restrict the resolution to $z \geq 0$. Since the equation is time reversible, this result can be easily extended to $z \leq 0$. We proceed into 3 steps.

Step 1. (Local well-posedness of the Cauchy problem.) Let $a_0 \in \mathbb{H}^m(\mathbb{R},\mathbb{C})$, with $m \geq 1$. To prove the local existence of a unique solution A to (1.9), we first transform it into an ODE in infinite dimension, with new unknown $V = \mathrm{e}^{-z\mathcal{D}}A$, solution of

$$\frac{\partial}{\partial z}V(z) = \mathcal{F}(z,V(z)) \qquad \forall z \in \mathbb{R}^+, \qquad V(0) = a_0,$$

where

$$\mathcal{F}(z,V) = \exp(-z\mathcal{D})\mathcal{N}_0(\exp(z\mathcal{D})V).$$

From Lemma 1.2 and Lemma 1.3, it can be directly deduced that $\mathcal{F}$ is locally Lipschitz continuous on $\mathbb{H}^m(\mathbb{R},\mathbb{C})$. More precisely, for all $M > 0$, there exists a constant $C_{m,M}$ such that, if $\|u\|_m \leq M$ and $\|v\|_m \leq M$, then

$$\forall z \in \mathbb{R}^+ \qquad \|\mathcal{F}(z,u) - \mathcal{F}(z,v)\|_m \leq C_{m,M}\|u-v\|_m.$$

The mapping $\mathcal{F}$ being also continuous on $\mathbb{R} \times \mathbb{H}^m(\mathbb{R},\mathbb{C})$, the Cauchy-Lipschitz theorem in Banach spaces gives the local existence of a unique maximal solution $V \in \mathcal{C}^1([0,Z[,\mathbb{H}^m(\mathbb{R},\mathbb{C}))$ such that

$$\text{if} \quad Z < +\infty \quad \text{then} \quad \limsup_{z\to Z} \|V(z)\|_m = +\infty.$$

Coming back to A, one has $A \in \mathcal{C}^0([0,Z[,\mathbb{H}^m(\mathbb{R},\mathbb{C}))$ and, by differentiating (1.9), one gets $A \in E_{m,N}([0,Z[)$. Moreover, since $\|A(z)\|_m = \|V(z)\|_m$, one has clearly

$$\text{if} \quad Z < +\infty \quad \text{then} \quad \limsup_{z\to Z} \|A(z)\|_m = +\infty. \tag{A.1}$$

In fact, the condition (A.1) can be replaced by (1.6). To prove this, we recall the following classical *tame estimate*, see [7]: for all $M > 0$, there exists $C_{m,M} > 0$ such that, for all $u \in \mathbb{H}^m(\mathbb{R},\mathbb{C})$ with $\|u\|_{\mathbb{L}^\infty} \leq M$, one has

$$\|\mathcal{N}_0(u)\|_m \leq C_{m,M}\|u\|_m. \tag{A.2}$$

Let us prove (1.6) by contradiction. We assume that $Z < +\infty$, together with

$$M = \|A\|_{\mathbb{L}^\infty((0,Z)\times\mathbb{R})} < +\infty.$$

From (A.2) and from the Duhamel formula

$$A(z) = \exp(z\mathcal{D})a_0 + \int_0^z \exp((z-\zeta)\mathcal{D})\mathcal{N}_0(A(\zeta))\,\mathrm{d}\zeta, \tag{A.3}$$

one gets

$$\|A(z)\|_m \leq \|a_0\|_m + \int_0^z \|\mathcal{N}_0(A(\zeta))\|_m \, \mathrm{d}\zeta \leq \|a_0\|_m + C_{m,M} \int_0^z \|A(\zeta)\|_m \, \mathrm{d}\zeta.$$

Hence, by the Gronwall lemma,

$$\forall z \in [0, Z[\qquad \|A(z)\|_m \leq e^{ZC_{m,M}} \|a_0\|_m,$$

which implies

$$\limsup_{z \to Z} \|A(z)\|_m < +\infty,$$

and then, by (A.1), $Z = +\infty$, which is a contradiction. The proof of (1.6) is complete.

Step 2. ($\mathbb{L}^2$ estimate.) Introduce the new unknown $U(z) = \mathrm{e}^{\frac{\alpha}{2}z} A(z)$, satisfying

$$\frac{\partial}{\partial z} U(z) = \mathcal{D}U(z) + \widetilde{\mathcal{N}}_0(U)(z) \qquad \forall z \in \mathbb{R}^+, \qquad U(0) = a_0, \tag{A.4}$$

where $\widetilde{\mathcal{N}}_0(U)(z) = \mathrm{i}\gamma \mathrm{e}^{-\alpha z} U(z)|U(z)|^2$. Multiplying (A.4) by $\mathrm{i}\,\overline{U}$ and integrating with respect to t, we obtain for the imaginary part

$$\Im\left(\mathrm{i} \int_{\mathbb{R}} \overline{U}(z)\, \partial_z U(z) \, \mathrm{d}t\right) = \frac{1}{2} \frac{d}{dz} \|U(z)\|_0^2 = 0$$

because $\Im(\mathrm{i}\partial_z U(z)\, \overline{U}(z)) = \Re(\partial_z U(z)\, \overline{U}(z)) = \frac{1}{2}\partial_z(U(z)\, \overline{U}(z))$. It follows that

$$\forall z \in [0, Z[\qquad \|U(z)\|_0 = \|a_0\|_0 \tag{A.5}$$

and therefore $\|A(z)\|_0 = \mathrm{e}^{-\frac{\alpha}{2}z} \|a_0\|_0$, which is (1.5).

Step 3. (A priori bound in $\mathbb{H}^N(\mathbb{R}, \mathbb{C})$ and global existence for $N = 2P$.) From now on, we assume that $N = 2P$, with $P \in \mathbb{N}^*$, and that $m \geq P$. To prove that $Z = +\infty$, by (1.6) it suffices to obtain an a priori estimate on the $\mathbb{H}^P(\mathbb{R}, \mathbb{C})$ norm of $U(z)$, which will imply an $\mathbb{L}^\infty$ estimate by Sobolev embeddings.

To prove that $\|U(z)\|_P$ is bounded, we derive a second conservation law for (A.4). Multiply (A.4) by $\mathrm{i}\partial_z \overline{U}(z)$ and integrate with respect to t. The real part reads, $\forall z \in [0, Z[$,

$$\Re\left(-\sum_{n=2}^{2P} \mathrm{i}^n \frac{\beta_n}{n!} \int_{\mathbb{R}} \partial_t^n U(z)\, \partial_z \overline{U}(z) \, \mathrm{d}t - \gamma \mathrm{e}^{-\alpha z} \int_{\mathbb{R}} |U(z)|^2\, U(z)\, \partial_z \overline{U}(z) \, \mathrm{d}t\right) = 0. \tag{A.6}$$

We set $I_n = -\int_{\mathbb{R}} \Re\left(\mathrm{i}^n \frac{\beta_n}{n!} \partial_t^n U(z)\, \partial_z \overline{U}(z)\right) \mathrm{d}t$. Using integrations by parts, respectively for $n = 2j$ and $n = 2j+1$, we obtain

$$I_{2j} = -\frac{\beta_{2j}}{2(2j)!} \frac{d}{dz} \int_{\mathbb{R}} |\partial_t^j U(z)|^2 \, \mathrm{d}t, \qquad I_{2j+1} = -\frac{\mathrm{i}\beta_{2j+1}}{2(2j+1)!} \frac{d}{dz} \int_{\mathbb{R}} \partial_t^j \overline{U}(z)\, \partial_t^{j+1} U(z) \, \mathrm{d}t.$$

The last part of equation (A.6) is rewritten as

$$\int_{\mathbb{R}} |U(z)|^2\, U(z)\, \partial_z \overline{U}(z)\, \mathrm{e}^{-\alpha z} \, \mathrm{d}t = \frac{1}{4} \frac{d}{dz} \int_{\mathbb{R}} |U(z)|^4\, \mathrm{e}^{-\alpha z} \, \mathrm{d}t + \frac{\alpha}{4} \int_{\mathbb{R}} |U(z)|^4\, \mathrm{e}^{-\alpha z} \, \mathrm{d}t.$$

Equation (A.6) then reads

$$-\frac{\partial}{\partial z}\mathcal{B}(z) - \frac{\gamma\alpha}{2}\int_{\mathbb{R}} |U(z)|^4\,\mathrm{e}^{-\alpha z}\,\mathrm{d}t = 0,$$

where

$$\begin{aligned}\mathcal{B}(z) = \sum_{j=1}^{P-1}\left(\frac{\beta_{2j}}{(2j)!}\int_{\mathbb{R}}|\partial_t^j U(z)|^2\,\mathrm{d}t + \mathrm{i}\frac{\beta_{2j+1}}{(2j+1)!}\int_{\mathbb{R}}\partial_t^{j+1}U(z)\,\partial_t^j\overline{U}(z)\,\mathrm{d}t\right)\\ + \frac{\beta_{2P}}{(2P)!}\int_{\mathbb{R}}|\partial_t^P U(z)|^2\,\mathrm{d}t + \frac{\gamma}{2}\int_{\mathbb{R}}|U(z)|^4\,\mathrm{e}^{-\alpha z}\,\mathrm{d}t. \end{aligned} \tag{A.7}$$

It follows that

$$\mathcal{B}(z) = \mathcal{B}(0) - \frac{\gamma\alpha}{2}\int_0^z\int_{\mathbb{R}}|U(\zeta)|^4\,\mathrm{e}^{-\alpha\zeta}\;\mathrm{d}t\;\mathrm{d}\zeta. \tag{A.8}$$

In particular, if the attenuation/gain coefficient α vanishes, then $\mathcal{B}$ is independent of z. Moreover, this identity implies that the mapping $z \in \mathbb{R}^+ \mapsto \mathcal{B}(z) \in \mathbb{R}$ is decreasing in the case $\alpha \geq 0$ and $\gamma \geq 0$.

Let us now derive from (A.8) an a priori bound of U in $\mathbb{H}^P(\mathbb{R},\mathbb{C})$, showing that $\mathcal{B}(z)$ is greater than a quantity depending on $\|\partial_t^P U(z)\|_0^2$. Using Gagliardo-Nirenberg inequality and Young inequality, we get for all $\varepsilon > 0$ and for all $(p_j, p_j') \in \mathbb{R}^+ \times \mathbb{R}^+$ such that $\frac{1}{p_j} + \frac{1}{p_j'} = 1$,

$$\left|\int_{\mathbb{R}}\partial_t^j\overline{U}(z)\,\partial_t^{j+1}U(z)\;\mathrm{d}t\right| \leq \frac{1}{p_j}\varepsilon^{p_j}\,\|\partial_t^P U(z)\|_0^{\frac{2j+1}{P}p_j} + \frac{1}{p_j'\varepsilon^{p_j'}}\,\|U(z)\|_0^{(2-\frac{2j+1}{P})p_j'}$$

which becomes, for $p_j = \frac{2P}{2j+1}$ and $p_j' = \frac{2P}{2P-2j-1}$,

$$\left|\int_{\mathbb{R}}\partial_t^j\overline{U}(z)\,\partial_t^{j+1}U(z)\;\mathrm{d}t\right| \leq \frac{1}{p_j}\varepsilon^{p_j}\|\partial_t^P U(z)\|_0^2 + \frac{1}{p_j'\varepsilon^{p_j'}}\|U(z)\|_0^2.$$

In the same way, with $q_j = \frac{P}{j}$ and $q_j' = \frac{P}{P-j}$ we obtain for all $\varepsilon > 0$

$$\int_{\mathbb{R}}\left|\partial_t^j U(z)\right|^2\;\mathrm{d}t \leq \frac{1}{q_j}\varepsilon^{q_j}\,\|\partial_t^P U(z)\|_0^2 + \frac{1}{q_j'\varepsilon^{q_j'}}\,\|U(z)\|_0^2.$$

Remark that, for all $j \leq P-1$, we have $1 < q_j, q_j', p_j, p_j' < +\infty$. Without loss of generality, we assume that $\beta_{2P} > 0$ (otherwise, change z to $-z$) and we choose ε small enough such that

$$\sum_{j=1}^{P-1}\left(\frac{|\beta_{2j}|}{(2j)!}\frac{1}{q_j}\varepsilon^{q_j} + \frac{|\beta_{2j+1}|}{(2j+1)!}\frac{1}{p_j}\varepsilon^{p_j}\right) \leq \frac{1}{2}\frac{\beta_{2P}}{(2P)!}.$$

Then, from (A.7) and the previous inequalities, we deduce that

$$\mathcal{B}(z) \geq \frac{1}{2}\frac{\beta_{2P}}{(2P)!}\|\partial_t^P U(z)\|_0^2 - C_1\|U(z)\|_0^2 + \frac{\gamma}{2}\int_{\mathbb{R}}|U(z)|^4\,\mathrm{e}^{-\alpha z}\;\mathrm{d}t$$

where $C_1 = \sum_{j=1}^{P-1}\left(\frac{|\beta_{2j}|}{(2j)!}\frac{1}{q_j'\varepsilon^{q_j'}} + \frac{|\beta_{2j+1}|}{(2j+1)!}\frac{1}{p_j'\varepsilon^{p_j'}}\right)$. Setting $C_2 = \frac{2(2P)!}{\beta_{2P}}$, it follows from (A.8) that

$$\begin{aligned}\|\partial_t^P U(z)\|_0^2 \leq & C_2\mathcal{B}(0) + C_1C_2\|U(z)\|_0^2\\ & - C_2\frac{\gamma}{2}\left(\int_{\mathbb{R}}|U(z)|^4\,\mathrm{e}^{-\alpha z}\;\mathrm{d}t + \alpha\int_0^z\int_{\mathbb{R}}|U(\zeta)|^4\,\mathrm{e}^{-\alpha\zeta}\;\mathrm{d}t\;\mathrm{d}\zeta\right).\end{aligned} \tag{A.9}$$

Next, the growth of $\|\partial_t^P U(z)\|_0$ can be controlled for all $z \in [0, Z[$ thanks to the Gagliardo-Nirenberg inequality

$$\int_{\mathbb{R}} |U(z)|^4 \mathrm{e}^{-\alpha z} \, \mathrm{d}t \leq \int_{\mathbb{R}} |U(z)|^4 \, \mathrm{d}t \leq C \|U(z)\|_0^{4-\frac{1}{P}} \|\partial_t^P U(z)\|_0^{\frac{1}{P}}.$$

From (A.9), we get

$$\begin{aligned}
\|\partial_t^P U(z)\|_0^2 \leq & C_2 \mathcal{B}(0) + C_1 C_2 \|U(z)\|^2 \\
& + C_3 \left(\|U(z)\|_0^{4-\frac{1}{P}} \|\partial_t^P U(z)\|_0^{\frac{2}{P}} + \int_0^z \|U(\zeta)\|_0^{4-\frac{1}{P}} \|\partial_t^P U(\zeta)\|_0^{\frac{2}{P}} \, \mathrm{d}\zeta \right) \\
\leq & C_4 + C_5 \left(\|\partial_t^P U(z)\|_0^{\frac{2}{P}} + \int_0^z \|\partial_t^P U(\zeta)\|_0^{\frac{2}{P}} \, \mathrm{d}\zeta \right)
\end{aligned}$$

where C_3, C_4 and C_5 are positive constants. The following version of Gronwall's lemma implies that $\|\partial_t^P U(z)\|_0$ is bounded on every finite interval $[0, L[\subset [0, Z[$ and then, that $\|U(z)\|_P$ is bounded on the same interval. This is enough to conclude that $Z = +\infty$ (if $Z < +\infty$, take $L = Z$). The proof of Theorem 1.1 is complete.

LEMMA A.1. *Let $a, b > 0$, m be a positive integer and y be a positive function with regularity $\mathcal{C}^1$ satisfying $y(t) \leq a + by(t)^{\frac{1}{m}} + b\int_0^t y(s)^{\frac{1}{m}} \, \mathrm{d}s$. Then $\forall t \in [0, T]$*

$$y(t) \leq \left((a + b\, y(0))^{1-\frac{1}{m}} + \frac{(m-1)}{m} \, b\, t + \frac{b(m-1)}{m^2} \, \ln\left(\frac{y(t)}{y(0)} \right) \right)^{m/(m-1)}.$$

Appendix B. The RK4-IP algorithm for solving the GNLSE.

RK4-IP algorithm

Input: Array u contains the input signal amplitude sampled over the time window.
Array $[\nu_j]_{j=1,\ldots,J}$ contains the frequency sampling points.
Array $[z_k]_{k=0,\ldots,K}$ contains the spatial grid points.
Array $\widehat{h}_R$ containing the sampling of the FT of the Raman response function.
{Initialisation}
for $j = 1, \ldots, J$ **do**
  $\widehat{d}[j] \leftarrow \mathrm{i} \sum_{n=2}^{N} \frac{\beta_n}{n!} (2\pi\nu_j)^n$
  $tfexpd[j] \leftarrow \exp(\frac{h}{2}\widehat{d}[j])$
end for
$\widehat{u}_1 \leftarrow \mathrm{FFT}(u, forward)$
{Loop over the propagation subinterval}
for $k = 1, \ldots, K$ **do**
  for $j = 1, \ldots, J$ **do**
    $\widehat{u}_{ip}[j] \leftarrow tfexpd[j] \times \widehat{u}_1[j]$
  end for
  $\widehat{\alpha}_1 \leftarrow \mathrm{COMPUTE\_TFN}(u, \widehat{u}_1)$
  for $j = 1, \ldots, J$ **do**
    $\widehat{\alpha}_1[j] \leftarrow tfexpd[j] \times \widehat{\alpha}_1[j]$
    $\widehat{u}_2[j] \leftarrow \widehat{u}_{ip}[j] + \frac{h}{2}\widehat{\alpha}_1[j]$
  end for
  $u_2 \leftarrow \mathrm{FFT}(\widehat{u}_2, backward)$
  $\widehat{\alpha}_2 \leftarrow \mathrm{COMPUTE\_TFN}(u_2, \widehat{u}_2)$

for $j = 1, \ldots, J$ **do**
$\widehat{u}_3[j] \leftarrow \widehat{u}_{ip}[j] + \frac{h}{2}\widehat{\alpha}_2[j]$
end for
$u_3 \leftarrow \mathrm{FFT}(\widehat{u}_3, backward)$
$\widehat{\alpha}_3 \leftarrow \mathrm{COMPUTE\_TFN}(u_3, \widehat{u}_3)$
for $j = 1, \ldots, J$ **do**
$\widehat{u}_4[j] \leftarrow tfexpd[j] \times (\widehat{u}_{ip}[j] + h\widehat{\alpha}_3[j])$
end for
$u_4 \leftarrow \mathrm{FFT}(\widehat{u}_4, backward)$
$\widehat{\alpha}_4 \leftarrow \mathrm{COMPUTE\_TFN}(u_4, \widehat{u}_4)$
for $j = 1, \ldots, J$ **do**
$\widehat{u}_1[j] \leftarrow tfexpd[j] \times (\widehat{u}_{ip}[j] + \frac{h}{6}\widehat{\alpha}_1[j] + \frac{h}{3}\widehat{\alpha}_2[j] + \frac{h}{3}\widehat{\alpha}_3[j]) + \frac{h}{6}\widehat{\alpha}_4[j]$
end for
$u \leftarrow \mathrm{FFT}(\widehat{u}_1, backward)$ {Array u contains the values $[A_k(z_{k+1}, t_j)]_{j=1,\ldots,J}$ the sampling of the signal amplitude at step z_k}
end for

$\mathrm{FFT}(u, forward)$ stands for a call to the Fast Fourier Transform (FFT) algorithm to compute the Discrete Fourier Transform (DFT) of array u, $\mathrm{FFT}(u, backward)$ stands for a call to FFT algorithm to compute the inverse DFT of array u, and COMPUTE_TFN refers to the following function.

FUNCTION $\widehat{g}$ = COMPUTE_TFN(f, $\widehat{f}$)
{Compute the Fourier Transform of $g : t \mapsto \mathcal{N}(f)(z,t)$ for a given z}
Input: Array f contains the time sampling of function f for the given z.
Array $\widehat{f}$ contains the sampled FT of f.
Array $[\nu_j]_{j=1,\ldots,J}$ contains the frequency sampling points.
Array $\widehat{h}_R$ containing the sampling of the FT of the Raman response function.
Output: Array $\widehat{g}$ contains the sampled FT of g.
for $j = 1, \ldots, J$ **do**
$op_1[j] \leftarrow |f[j]|^2$
end for
$\widehat{op}_1 \leftarrow \mathrm{FFT}(op_1, forward)$
for $j = 1, \ldots, J$ **do**
$\widehat{op}_2[j] \leftarrow \widehat{op}_1[j] \times \widehat{h}_R[j]$
end for
$op_2 \leftarrow \mathrm{FFT}(\widehat{op}_2, backward)$ {Array op_2 contains the convolution product $h_R \star |f|^2$}
for $j = 1, \ldots, N$ **do**
$op_3[j] \leftarrow f[j] \times \big((1 - f_R)op_1[j] + f_R\, op_2[j]\big)$
end for
$\widehat{op}_3 \leftarrow \mathrm{FFT}(\widehat{op}_3, forward)$
for $j = 1, \ldots, J$ **do**
$\widehat{op}_4[j] \leftarrow \mathrm{i}\gamma(1 - \frac{2\mathrm{i}\pi\nu_j}{\omega_0})\widehat{op}_3[j]$
end for
for $j = 1, \ldots, J$ **do**
$\widehat{g}[j] \leftarrow -\frac{\alpha}{2}\widehat{f}[j] + \widehat{op}_4[j]$
end for

The computational cost in the above algorithm mainly lies in the computation of the Fourier Transforms. Over one spatial step, the number of Fourier Transforms is 16. The C

language program we have developed to solve the GNLSE (1.1) by the RK4-IP method uses the FFTW library for computing the Fourier Transforms [16].

Appendix C. The S3F-RK4 algorithm for solving the GNLSE.

S3F-RK4 algorithm

Input: Array u contains the input signal amplitude sampled over the time window .
Array $[\nu_j]_{j=1,\dots,J}$ contains the frequency sampling points.
Array $[z_k]_{k=0,\dots,K}$ contains the spatial grid points.
Array $\widehat{h}_R$ containing the sampling of the FT of the Raman response function.
{Initialisations}
for $j = 1, \dots, N$ **do**
$\widehat{d}[j] \leftarrow \mathrm{i} \sum_{n=2}^{N} \frac{\beta_n}{n!} (2\pi\nu_j)^n$
$tfexpd[j] \leftarrow \exp(\frac{h}{2}\widehat{d}[j])$
end for
$\widehat{u}_0 \leftarrow \mathrm{FFT}(u, forward)$
{Loop over the propagation subinterval}
for $k = 1, \dots, K$ **do**
for $j = 1, \dots, N$ **do**
$\widehat{u}_1[j] \leftarrow tfexpd[j] \times \widehat{u}_0[j]$
end for
$u_1 \leftarrow \mathrm{FFT}(\widehat{u}_1, backward)$
$\widehat{\alpha}_1 \leftarrow \mathrm{COMPUTE\_TFN}(u_1, \widehat{u}_1)$
for $j = 1, \dots, N$ **do**
$\widehat{u}_2[j] \leftarrow \widehat{u}_1[j] + \frac{h}{2}\widehat{\alpha}_1[j]$
end for
$u_2 \leftarrow \mathrm{FFT}(\widehat{u}_2, backward)$
$\widehat{\alpha}_2 \leftarrow \mathrm{COMPUTE\_TFN}(u_2, \widehat{u}_2)$
for $j = 1, \dots, N$ **do**
$\widehat{u}_3[j] \leftarrow \widehat{u}_1[j] + \frac{h}{2}\widehat{\alpha}_2[j]$
end for
$u_3 \leftarrow \mathrm{FFT}(\widehat{u}_3, backward)$
$\widehat{\alpha}_3 \leftarrow \mathrm{COMPUTE\_TFN}(u_3, \widehat{u}_3)$
for $j = 1, \dots, N$ **do**
$\widehat{u}_4[j] \leftarrow \widehat{u}_1[j] + h\widehat{\alpha}_3[j]$
end for
$u_4 \leftarrow \mathrm{FFT}(\widehat{u}_4, backward)$
$\widehat{\alpha}_4 \leftarrow \mathrm{COMPUTE\_TFN}(u_4, \widehat{u}_4)$
for $j = 1, \dots, N$ **do**
$\widehat{u}_0[j] \leftarrow tfexpd[j] \times (\widehat{u}_1[j] + \frac{h}{6}\widehat{\alpha}_1[j] + \frac{h}{3}\widehat{\alpha}_2[j] + \frac{h}{3}\widehat{\alpha}_3[j] + \frac{h}{6}\widehat{\alpha}_4[j])$
end for
{The following line can be removed when only the solution at the fiber end is required and placed after the loop}
$u \leftarrow \mathrm{FFT}(\widehat{u}_0, backward)$
end for

The function COMPUTE_TFN(f, $\widehat{f}$) is given on p. 23.

One may observe the very similar form of both the RK4-IP and S3F-RK4 algorithms. In particular, their respective cost is comparable since both require the computation of 16 FT per step (one more for S3F-RK4 if the solution is required for each step z_k and not only at the end of the fiber).

REFERENCES

[1] G. Agrawal. *Nonlinear fiber optics*. Academic Press, 3rd edition, 2001.

[2] L. Auslander and F.A. Grunbaum. The Fourier transform and the discrete Fourier transform. *Inverse Probl.*, 5(2):149–164, 1989.

[3] S. Balac and F. Mahé. Embedded Runge-Kutta scheme for step-size control in the Interaction Picture method. *Comput. Phys. Commun.*, 184:1211–1219, 2013.

[4] C. Besse, B. Bidégaray, and S. Descombes. Order estimates in time of splitting methods for the nonlinear Schrödinger equation. *SIAM J. Numer. Anal.*, 40(1):26–40, 2002.

[5] J.C. Butcher. *Numerical methods for ordinary differential equations*. John Wiley and Sons, 2008.

[6] B.M. Caradoc-Davies. *Vortex dynamics in Bose-Einstein condensate*. PhD thesis, University of Otago (NZ), 2000.

[7] R. Carles. Semi-classical analysis for nonlinear Schrödinger equations. World Scientific Publishing Co. Pte. Ltd., Hackensack, NJ, 2008.

[8] T. Cazenave. *Semilinear Schrödinger Equations*. Courant Lecture Notes in Mathematics, AMS, New York, 2003.

[9] T. Cazenave and A. Haraux. *Introduction aux problèmes d'évolution semi-linéaires*. Ellipses, 1990.

[10] M. Crouzeix and A. Mignot. *Analyse numérique des équations différentielles*. Masson, Paris, 1984.

[11] M.J. Davis. *Dynamics in Bose-Einstein condensate*. PhD thesis, University of Oxford (UK), 2001.

[12] J.R. Dormand and P.J. Prince. A family of embedded Runge-Kutta formulae. *J. Comput. Appl. Math.*, 6:19–26, 1980.

[13] G. Dujardin. Exponential Runge-Kutta methods for the Schrödinger equation. *Appl. Numer. Math.*, 59:1839–1857, 2009.

[14] C.L. Epstein. How well does the finite Fourier transform approximate the Fourier transform? *Comm. Pure Appl. Math.*, 58(10):1421–1435, 2005.

[15] A. Fernandez, S. Balac, A. Mugnier, F. Mahé, R. Texier-Picard, T. Chartier, and D. Pureur. Numerical simulation of incoherent optical wave propagation in nonlinear fibers. *To appear in Eur. Phys. J. - Appl. Phys.*, 2013.

[16] M. Frigo and S.G. Johnson. The design and implementation of FFTW3. *P. IEEE*, 2(93):216–231, 2005.

[17] M. Guenin. On the interaction picture. *Commun. Math. Phys.*, 3:120–132, 1966.

[18] E. Hairer, S. P. Norsett, and G. Wanner. *Solving ordinary differential equations I: nonstiff problems*. Springer-Verlag New York, Inc., New York, NY, USA, 1993.

[19] A. Heidt. Efficient adaptive step size method for the simulation of supercontinuum generation in optical fibers. *J. Lightwave Technol.*, 27(18):3984–3991, 2009.

[20] J. Hult. A fourth-order Runge–Kutta in the Interaction Picture method for simulating supercontinuum generation in optical fibers. *J. Lightwave Technol.*, 25(12):3770–3775, 2007.

[21] C.-N. Liu, G. G. Krishna, M. Umetsu, and S. Watanabe. Numerical investigation of contrast degradation of Bose-Einstein condensate interferometers. *Phy. Rev. A*, 79(1), 2009.

[22] C. Lubich. On splitting methods for Schrödinger-Poisson and cubic nonlinear Schrödinger equations. *Math. Comp.*, 77:2141–2153, 2008.

[23] A. Ostermann M. Hochbruck. Explicit exponential Runge-Kutta methods for semilinear parabolic problems. *SIAM J. Numer. Anal.*, 43:1069–1090, 2005.

[24] A. Ostermann M. Hochbruck. Exponential Runge-Kutta methods for parabolic problems. *Appl. Numer. Math.*, 53:323–339, 2005.

[25] R.I. McLachlan and G.R.W. Quispel. Splitting methods. *Acta Numer.*, 11:341–434, 2002.

[26] K. Okamoto. *Fundamentals of Optical Waveguides*. Optics and Photonics. Elsevier, 2006.

[27] R. Scott, C. Gardiner, and D. Hutchinson. Nonequilibrium dynamics: Studies of the reflection of Bose-Einstein condensates. *Laser Phys.*, 17:527–532, 2007.

[28] O.V. Sinkin, R. Holzlöhner, J. Zweck, and C.R. Menyuk. Optimization of the Split-Step Fourier method in modeling optical-fiber communications systems. *J. Lightwave Technol.*, 21(1):61, 2003.

[29] G. Strang. On the construction and comparison of difference schemes. *SIAM J. Numer. Anal.*, 5(3):506–517, 1968.

[30] J.S. Townsend. *A modern approach to quantum mechanics*. International series in pure and applied physics. University Science Books, 2000.

[31] J.A.C. Weideman and B.M. Herbst. Split-step methods for the solution of the nonlinear Schrodinger equation. *SIAM J. Numer. Anal.*, 23(3):485–507, 1986.

[32] S. Wüster, T. E. Argue, and C. M. Savage. Numerical study of the stability of skyrmions in Bose-Einstein condensates. *Phys. Rev. A*, 72(4), 2005.